

Manuscript Number: QUAGEO-D-16-00005R1

Title: AN APPROACH FOR OPTIMIZING IN SITU COSMOGENIC  $^{10}\text{Be}$  SAMPLE PREPARATION

Article Type: Research Paper

Keywords: geomorphology; Earth surface process; geochronology; cosmogenic nuclides; sample preparation

Corresponding Author: Ms. Lee B Corbett,

Corresponding Author's Institution: University of Vermont

First Author: Lee B Corbett

Order of Authors: Lee B Corbett; Paul R Bierman; Dylan H Rood

Abstract: Optimizing sample preparation for the isotopic measurement of  $^{10}\text{Be}$  extracted from quartz mineral separates has a direct positive effect on the efficiency of sample production and the accuracy and precision of isotopic analysis. Here, we demonstrate the value of tracing Be throughout the extraction process (both after dissolution and after processing), producing pure Be (by optimizing column chromatography methods and quantifying quartz mineral separate purity), and minimizing backgrounds (through reducing both laboratory process blanks and  $^{10}\text{B}$  isobaric interference). These optimization strategies increase the amount of  $^{10}\text{Be}$  available for analysis during accelerator mass spectrometry (AMS), while simultaneously decreasing interference and contamination, and ensuring that sample performance matches standard performance during analysis. After optimization of our laboratory's extraction methodology,  $^{9}\text{Be}^{3+}$  beam currents, a metric for sample purity and Be yield through the extraction process, matched the  $^{9}\text{Be}^{3+}$  beam currents of AMS standards analyzed at the same time considering nearly 800 samples. Optimization of laboratory procedures leads to purer samples that perform better, more consistently, and more similarly to standards during AMS analysis, allowing for improved dating and quantification of Earth surface processes.

The University of Vermont

DEPARTMENT OF GEOLOGY  
DELAHANTY HALL  
180 COLCHESTER AVENUE  
BURLINGTON, VERMONT 05405-1758  
(802) 656-3396  
FAX (802) 656-0045



February 2, 2016

To the Editor:

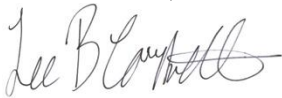
After performing the revisions suggested by two reviewers, we are resubmitting our manuscript, **An Approach for Optimizing *In Situ* Cosmogenic  $^{10}\text{Be}$  Sample Preparation**, for publication in *Quaternary Geochronology*.

We appreciated the comments from both reviewers and found that their suggestions improved the manuscript. In our revisions, we focused particular attention toward broadening our discussion of measurement accuracy, clarifying the impact of Ti impurities in samples, providing more information about beam current normalization, and benchmarking our methods against those previously used in our laboratory. As a group, we considered each suggestion and addressed it in the way that we thought most benefited the manuscript. In the following pages, you will find a list of the reviewers' suggestions and details about how we incorporated those suggestions.

We are optimistic that our revisions have addressed the reviewers' concerns and that the manuscript has grown in both clarity and applicability. Thank you in advance for considering our revised draft.

Sincerely,

Lee Corbett (for the author team)



Department of Geology and Rubenstein School of Environment and Natural Resources  
University of Vermont  
180 Colchester Ave, Burlington VT 05405  
Ashley.Corbett@uvm.edu  
(802) 380-2344

*Please note: Our responses below are in red.*

Ms. Ref. No.: QUAGEO-D-16-00005

Title: AN APPROACH FOR OPTIMIZING IN SITU COSMOGENIC <sup>10</sup>BE SAMPLE PREPARATION

Quaternary Geochronology

Comments from Reviewer #1

The paper of Corbett et al. describes in detail the chemical separation procedure for Be-10 in quartz samples applied at the University of Vermont. They show how their column chemistry was optimized for the purification of Be and they impressively demonstrate, on the statistical base of about 800 samples, that their lab constantly produces high quality Be-10 samples. This paper is important not only for newcomers in the field, e.g. who want to set up their own lab, but also for the existing cosmo labs because it demonstrates the importance of quality control e.g. to avoid systematic errors in the final Be-10 ages. Despite the mainly descriptive nature of the paper (comparable to a status report of the lab), I still believe it is worth being published in QG mainly because of the very detailed discussion of their procedures and the (basic) statistical analysis of their data. I therefore support publication in QG after minor revisions. A detailed list of comments (ordered as they would appear in the text) is given below.

*We thank the Reviewer for the positive feedback and are glad to hear that the paper will be of use to members of the cosmogenic nuclide community. We have purposefully tried to make the techniques described in the manuscript generalizable to a wide range of laboratories and AMS systems so that the central theme of quality control can be applied throughout the community.*

Page 4, line 11: "The accuracy of sample measurement is controlled in part by how closely sample performance matches standard performance during AMS analysis. "

I agree, but in a strict sense this is only true if the AMS system shows a current dependency (i.e. a correlation between current of the stable isotope and the measured isotopic ratio). Further, this picks out one possible factor influencing the accuracy. Other possibilities should be mentioned, e.g. matrix effects (stds do not go through sample chemistry).

*We agree that accuracy is dictated by numerous factors and that we did not give sufficient attention to these factors in the initial draft of the manuscript. We have rewritten the paragraph in question (fourth paragraph of the introduction) to have a broader focus. Rather than solely discussing beam currents, we begin with a more general discussion of accuracy that includes some of the ideas mentioned by the Reviewer. We then narrow the focus to beam currents toward the end of the paragraph, since this is the metric we assess with our dataset.*

Page 4, line 23: The total number of attainable counts is a product of the <sup>10</sup>Be concentration of the material being analyzed, the TOTAL MASS OF THE SAMPLE, and the AMS total system efficiency (including ionization, transmission, transport AND DETECTION efficiencies).

*Change made- we reworded the sentence as suggested.*

Page 6, line 16: I think it would be appropriate to refer to G. Raisbeck's work here, since he is one of the pioneers of Be-10.

We thank the Reviewer for pointing out this important omission and have added two references to Raisbeck's pioneering work in this section.

Page 7, lines 12-16: I was hoping that this study could/would shed some light on the myth that Ti is "poisoning" the ion source. Obviously the data of the authors provides no support for this. It would have been nice to see some performance data, e.g. same sample with and without Ti removal.

We do not think we are able to assess the "Ti myth" with the data we present here, although we agree that this would be a useful targeted study to perform. As described in the manuscript, we remove Ti from all samples; in the rare instances where Ti remains in the post-processing aliquots, we reprocess the sample to remove the remaining Ti. Thus our dataset does not represent a range of Ti concentrations against which we can assess beam current variability. A different study design (perhaps samples spiked with varying amounts of Ti?) could address this question, but is outside the scope of this manuscript. Please see the additional comment about Ti below for more detail about how these ideas have been incorporated into the revised version of the manuscript. Note also that this question has been addressed in the University of Vermont lab previously, as described in Hunt et al. (2008), where Ti was found to be a source poison. It is because of the findings presented in Hunt et al. (2008), which we reference in our manuscript, that we strive to remove all Ti from samples.

Page 9, lines 6ff: I do not understand the normalization procedure. Is the total average sample current normalized to the current of the standard during the first pass? Or do you take the first pass from both only? If yes, why?

We agree that the normalization procedure was not fully described in the first draft of the manuscript. The sample beam currents we present are the averages of the first two 300-second counting cycles. We chose this procedure since samples were counted between two and four times and we wanted to chose a method that would be consistent between all samples. We have added this material to the paragraph in question.

Page 17f: Discussion: In this section I'm missing references to the Figures you are discussing. It is not always immediately clear whether you are discussing part a) or b) of a Figure in the text (e.g. Fig 5b on page 17 line 17ff).

We have added additional figure references to the location identified here. We also went through the Discussion carefully and added figure references in several other locations in order to enhance clarity.

Page 20, line 1ff: Again the Ti-myth - can't you (dis)prove this with your data?

Please see our above response about Ti. We do not think our dataset can address this question and have added a sentence to this effect at the end of the paragraph. However, this question has already been explored in the University of Vermont laboratory and was detailed in Hunt et al. (2008).

Figure 10b: The normalized current should be without units.

Change made- we have removed the units from the x-axis of the normalized current plot.

### Comments from Reviewer #3

The paper is a pure methodology paper on the optimisation of already existing chemical processes for the isolation of a long-lived radionuclide.

I would like to suggest to reject the paper for Quaternary Geochronology mainly because it better fits to be published in a real radiochemistry journal such as Radiochim. Acta, Journal of Radioanalytical and Nuclear Chemistry or Applied Radiation and Isotopes.

There the editors and reviewers have probably the best knowledge to decide if the presented "new" chemistry or as the authors correctly say in their title "AN APPROACH FOR OPTIMIZING" is worth its own scientific publication.

There are multiple possible outlets for this manuscript, but we chose Quaternary Geochronology specifically for its broad readership base. There are now over 30 cosmogenic nuclide sample preparation laboratories in the United States alone, and many more abroad, and we feel confident that some of these laboratories may benefit from implementing any combination of the techniques we describe here. The reality is that most of the faculty running these preparation labs are one or several generations behind the pioneers of cosmogenic nuclide studies, and thus may not read the highly-technical, radio-nuclide focused, or AMS-specific journals that their predecessors did. Since cosmogenic nuclide studies are growing so rapidly, and we feel strongly that data quality and efficiency are important, our goal with submitting to Quaternary Geochronology was to reach the entire cosmogenic community rather than just the most technically-minded portion.

However, from my basic radiochemistry experience, I would judge that it might not contain enough "new stuff" to justify its own publication without testing for several samples (by taking Be-9 currents of samples and Be-10/Be-9 of processing blanks as quality indicators) the described chemistry versus an "old" but sophisticated chemistry. There is no real proof from AMS-data that the "new" chemistry is superior to the already applied ones at other AMS-facilities.

We thank the Reviewer for bringing up the idea of comparison of sample performance metrics between different processing approaches; this is an idea we considered ourselves multiple times during the writing process. Ultimately, we decided to avoid comparison with other laboratories, as we did not feel that it was our place to assess another laboratories' data quality. Rather, we chose to focus solely on our own development and optimization, benchmarking our progress against an earlier study of our laboratory methods (see Hunt et al., 2008). To address the comparison between our old and new methods more explicitly, we added a paragraph to Section 5.5 ("Sample Beam Currents") in the Results section. In this new paragraph, we compare the variability of beam currents using our new procedures to the variability of beam currents using older procedures in the University of Vermont laboratory (as presented in Hunt et al., 2008).

AN APPROACH FOR OPTIMIZING IN SITU COSMOGENIC  $^{10}\text{Be}$  SAMPLE  
PREPARATION

Lee B. Corbett<sup>1\*</sup>  
Paul R. Bierman<sup>1</sup>  
Dylan H. Rood<sup>2,3</sup>

<sup>1</sup> Department of Geology and Rubenstein School of the Environment and Natural Resources, University of Vermont, Burlington VT 05405, USA

<sup>2</sup> Department of Earth Science and Engineering, Imperial College London, South Kensington Campus, London SW7 2AZ, UK

<sup>3</sup> Center for Accelerator Mass Spectrometry, Lawrence Livermore National Laboratory, Livermore CA 94550, USA

\* *Contact author: Ashley.Corbett@uvm.edu, 802-380-2344*

1 **Abstract**

2 Optimizing sample preparation for the isotopic measurement of  $^{10}\text{Be}$  extracted from quartz  
3 mineral separates has a direct positive effect on the efficiency of sample production and the  
4 accuracy and precision of isotopic analysis. Here, we demonstrate the value of tracing Be  
5 throughout the extraction process (both after dissolution and after processing), producing pure  
6 Be (by optimizing column chromatography methods and quantifying quartz mineral separate  
7 purity), and minimizing backgrounds (through reducing both laboratory process blanks and  $^{10}\text{B}$   
8 isobaric interference). These optimization strategies increase the amount of  $^{10}\text{Be}$  available for  
9 analysis during accelerator mass spectrometry (AMS), while simultaneously decreasing  
10 interference and contamination, and ensuring that sample performance matches standard  
11 performance during analysis. After optimization of our laboratory's extraction methodology,  
12  $^9\text{Be}^{3+}$  beam currents, a metric for sample purity and Be yield through the extraction process,  
13 matched the  $^9\text{Be}^{3+}$  beam currents of AMS standards analyzed at the same time considering nearly  
14 800 samples. Optimization of laboratory procedures leads to purer samples that perform better,  
15 more consistently, and more similarly to standards during AMS analysis, allowing for improved  
16 dating and quantification of Earth surface processes.

17  
18 Keywords: geomorphology; Earth surface process; geochronology; cosmogenic nuclides; sample  
19 preparation

1 **1. Introduction**

2 Measurement of *in situ* produced cosmogenic  $^{10}\text{Be}$  in geologic samples provides insight  
3 about a wide variety of geologic processes (Bierman and Nichols, 2004; Gosse and Phillips,  
4 2001; Granger et al., 2013; Nishiizumi et al., 1993; von Blanckenburg and Willenbring, 2014).  
5 For example, quantifying  $^{10}\text{Be}$  concentrations in moraine boulders (Heyman et al., 2011; Phillips  
6 et al., 1990) or previously-glaciated bedrock surfaces (Bierman et al., 1999) provides information  
7 about past glacial behavior, thus yielding valuable paleoclimatic insight (Balco, 2011; Fabel and  
8 Harbor, 1999). Cosmogenic  $^{10}\text{Be}$  is useful for measuring displacement rates on fault systems by  
9 dating offset landforms (Bierman et al., 1995; Brown et al., 1998; Matmon et al., 2005; Rood et  
10 al., 2010). It can also be employed to study landscape erosion rates, both on outcrop scales  
11 (Nishiizumi et al., 1991; Nishiizumi et al., 1986) and basin scales (Bierman and Steig, 1996;  
12 Brown et al., 1995; Granger et al., 1996; von Blanckenburg, 2005), thereby providing insight  
13 about Earth's changing surface (Portenga and Bierman, 2011).

14 Cosmogenic  $^{10}\text{Be}$  forms *in situ* when high-energy cosmic rays bombard rock in the  
15 upper-most few meters of Earth's surface (Lal, 1988). In the mineral quartz,  $^{10}\text{Be}$  is produced  
16 primarily by spallation of oxygen at low rates, on the order of  $\sim 4$  atoms  $\text{g}^{-1}$  quartz  $\text{yr}^{-1}$  at sea level  
17 and high latitude (Balco et al., 2008). Production of  $^{10}\text{Be}$  in rock and soil is primarily dependent  
18 on latitude and elevation, and effectively ceases if the sample surface is buried to a depth of more  
19 than a few meters (for example, by glacial ice, sediment, or soil).  $^{10}\text{Be}$  has a half-life of  $\sim 1.4$   
20 million years (Chmeleff et al., 2010; Korschinek et al., 2010; Nishiizumi et al., 2007). Therefore,  
21 while concentrations of  $^{10}\text{Be}$  initially increase in exposed rock over time, they eventually level  
22 off as production, erosion, and decay reach steady state.



1           Preparing and analyzing a sample for  $^{10}\text{Be}$  measurement requires numerous steps. After a  
2 sample is collected, the mineral quartz is isolated from the other mineral phases through a series  
3 of physical and chemical processes (Kohl and Nishiizumi, 1992). The quartz is then dissolved in  
4 the presence of a  $^9\text{Be}$  carrier solution, and Be is chemically isolated. To measure  $^{10}\text{Be}$ , atoms of  
5 this rare isotope are counted in relation to the ion current of stable  $^9\text{Be}$  via accelerator mass  
6 spectrometry, or AMS (Muzikar et al., 2003; Tuniz et al., 1998). Because isotopic fractionation  
7 can occur in the AMS, primary standards such as the 07KNSTD dilution series (Nishiizumi et  
8 al., 2007) are analyzed in association with samples. A correction factor for the measured versus  
9 the assumed  $^{10}\text{Be}/^9\text{Be}$  ratio of primary standards is determined, then applied to samples analyzed  
10 at the same time.

11           The accuracy of sample measurement is controlled in part by the overall closeness of  
12 match between standards and samples. Developing a correction factor from standard  $^{10}\text{Be}/^9\text{Be}$   
13 ratios and using it to scale sample  $^{10}\text{Be}/^9\text{Be}$  ratios relies upon the assumption that standards and  
14 samples behave similarly during measurement. Important characteristics may include matrix  
15 effects (e.g. accessory elements that could interfere with measurement; Hunt et al. (2008),  
16 Merchel et al. (2008)), cathode geometry (e.g. depth to the sputtering surface and shape of the  
17 surface; Hunt et al. (2007), Rood et al. (2010), Shanks and Freeman (2015)), total mass, and  
18 performance during measurement (the ion source yield, or “beam current”, which we measure as  
19 the  $^9\text{Be}^{3+}$  current but which can alternatively be measured as the  $^9\text{Be}^{16}\text{O}^-$  current). The similarity  
20 of beam currents between standards and samples across multiple measurement cycles is  
21 particularly important (Rood et al., 2014). Additionally, contamination of a sample with the  
22 isobar  $^{10}\text{B}$ , above the ability of the detector to reject such interference, inhibits reliable detection  
23 of  $^{10}\text{Be}$  and has the potential to degrade accuracy (Merchel et al., 2012).

1           The precision of low  $^{10}\text{Be}/^9\text{Be}$  samples is primarily controlled by Poisson counting  
2 statistics, with greater numbers of  $^{10}\text{Be}$  counts yielding more precise analyses. The total number  
3 of attainable counts is a product of the  $^{10}\text{Be}$  concentration of the material being analyzed, the  
4 total mass of the sample, and the AMS total system efficiency (including ionization,  
5 transmission, transport, and detection efficiencies), all of which dictate the number of  $^{10}\text{Be}$   
6 counts that can be obtained before the sample material is ablated away during sputtering (Rood  
7 et al., 2013; Rood et al., 2010). For higher  $^{10}\text{Be}/^9\text{Be}$  samples, precision is primarily controlled by  
8 the reproducibility of ratio measurements, which is often poorer than that predicted by counting  
9 statistics alone (Rood et al., 2013). For these higher  $^{10}\text{Be}/^9\text{Be}$  samples that are limited by  
10 reproducibility rather than counting statistics, closeness of match to standards dictates precision  
11 in addition to accuracy (Rood et al., 2014). Background levels of  $^{10}\text{Be}$  introduced during sample  
12 processing also control the precision of measured isotopic ratios, with relatively higher process  
13 blanks increasing the uncertainty of sample  $^{10}\text{Be}/^9\text{Be}$  ratios especially in samples with little  $^{10}\text{Be}$ ,  
14 because background uncertainties are typically added in quadrature.

15           There are several reasons why it is advantageous to optimize the preparation of samples  
16 for  $^{10}\text{Be}$  isotopic analysis. Ensuring that sample performance matches standard performance  
17 during AMS analysis likely increases the accuracy of sample measurements, a prerequisite for  
18 accurate determination of dates and rates across a variety of applications. Increasing the  
19 precision of analyses enhances not only the interpretations that can be made from dates and rates,  
20 but also enables approaches involving multiple isotopic systems such as burial dating (Granger  
21 and Muzikar, 2001) and burial isochron dating (Balco and Rovey, 2008), and allows for  
22 improved calibration of cosmogenic nuclide production rates (Balco et al., 2009; Borchers et al.,  
23 2015; Briner et al., 2012; Putnam et al., 2010). Very low concentration samples, such as those

1 from young exposures (Licciardi et al., 2009), rapidly eroding landscapes (Portenga et al., 2015),  
2 or long-buried sediments (Erlanger et al., 2012; Gibbon et al., 2014), require low detection limits  
3 to be measurable above background levels. High  ${}^9\text{Be}^{3+}$  beam currents reduce the counting times  
4 required to achieve desired precisions, thereby speeding AMS throughput and better utilizing the  
5 limited beam time available for analysis.

6 This paper discusses optimization of the Be extraction procedure (Fig. 1) used at the  
7 University of Vermont, with the aim of increasing data accuracy and precision as well as the  
8 efficiency of sample preparation and AMS analysis. Our goal is to produce pure samples of Be  
9 that match the performance of standards, with particular focus on obtaining high Be yield,  
10 consistent  ${}^9\text{Be}^{3+}$  beam currents, low  ${}^{10}\text{Be}/{}^9\text{Be}$  background levels, and minimal isobaric  
11 interference. The optimization strategies discussed here are generalizable to other laboratories as  
12 well as to other AMS facilities.

13

## 14 **2. Brief History of ${}^{10}\text{Be}$ Extraction and Measurement**

15 Over time, different methods have been used to measure cosmogenic  ${}^{10}\text{Be}$ . Initially,  
16 abundances of cosmogenic  ${}^{10}\text{Be}$  were quantified by radioactive decay counting after Be was  
17 isolated from silicate minerals by dissolution in acid (Fairhall, 1960). However, only samples  
18 with the highest  ${}^{10}\text{Be}$  concentrations, for example those exposed at high elevations for long  
19 durations, could be measured. Later, it became possible to measure  ${}^{10}\text{Be}/{}^9\text{Be}$  ratios via AMS  
20 (Lanford et al., 1980; Raisbeck et al., 1978; Southon et al., 1983; Thomas et al., 1981; Turekian  
21 et al., 1979), including on lower-energy AMS systems (Raisbeck et al., 1987). Be yields from  
22 chemical preparation were typically high (85-90%), but samples frequently retained impurities,

1 especially Al (Lanford et al., 1980). At that time, precisions were generally 5-10%, and detection  
2 was limited to  $^{10}\text{Be}/^9\text{Be}$  ratios greater than  $\sim 10^{-13}$  (Southon et al., 1983).

3         Although measurements of  $^{10}\text{Be}$  became more common into the 1980's, average AMS  
4 beam currents remained relatively low (Klein and Middleton, 1984). By 1990, the quality of  
5 AMS measurements of  $^{10}\text{Be}$  increased, and precisions of several percent were attainable (Suter,  
6 1990). At around the same time, *in situ*  $^{10}\text{Be}$  became a more widely used dating technique as  
7 AMS analysis improved and after it was confirmed that meteoric  $^{10}\text{Be}$  produced in the  
8 atmosphere and adhered to the surface of grains could be removed from the grain coatings of a  
9 sample with repeated acid etches (Brown et al., 1991; Kohl and Nishiizumi, 1992; Nishiizumi et  
10 al., 1991; Nishiizumi et al., 1986; Nishiizumi et al., 1989). Adding column chromatography to  
11 the extraction protocol ensured that Be could be cleanly separated from other elements  
12 (Ditchburn and Whitehead, 1994; Tera et al., 1986).

13         Recent methodological advances have further increased the quality of AMS  $^{10}\text{Be}$   
14 measurements by improving beam currents. BeO had traditionally been mixed with Ag before  
15 being packing into cathodes for AMS analysis; however, using Nb instead of Ag increased  $^9\text{Be}^{3+}$   
16 beam currents (Hunt et al., 2006; Merchel et al., 2008). It is uncertain whether impurities in the  
17 final Be fraction decrease AMS  $^9\text{Be}^{3+}$  beam currents beyond dilution effects. Merchel et al.  
18 (2008) suggested that additions of Ti did not directly decrease  $^9\text{Be}^{3+}$  beam currents, although the  
19 resulting dilution of Be did. However, Hunt et al. (2008) found that Al and Ti both depressed  
20  $^9\text{Be}^{3+}$  beam currents beyond the effects of dilution (although Ca, Fe, Mg, and Mn did not).

21         Detection limits have also improved over the past several decades. The discovery that  
22 commercial aluminum often contains non-negligible amounts of  $^{10}\text{Be}$  occasioned the use of  
23 stainless steel and copper cathodes for sample analysis (Middleton et al., 1994), lowering

1 backgrounds. Although commercially-available  $^9\text{Be}$  carrier is commonly used, its  $^{10}\text{Be}/^9\text{Be}$  ratio  
2 is  $\sim 10^{-14}$ , which hinders the analysis of low-level samples. In contrast,  $^9\text{Be}$  carriers made from  
3 deeply-mined phenakite ( $\text{Be}_2\text{SiO}_4$ ) and beryl ( $\text{Be}_3\text{Al}_2\text{Si}_6\text{O}_{18}$ ) often yield  $^{10}\text{Be}/^9\text{Be}$  ratios two  
4 orders of magnitude lower (Merchel et al., 2008), which are better suited for the analysis of low-  
5 level samples. Experiments at Lawrence Livermore National Laboratory suggests that the AMS  
6 detection limit is now as low as  $\sim 1000$  total  $^{10}\text{Be}$  atoms in a sample (or  $\sim 10$   $^{10}\text{Be}$  counts,  
7 assuming a 1% total AMS efficiency) as long as backgrounds are low, making it possible to  
8 obtain high-precision measurements on small samples or samples with little  $^{10}\text{Be}$  (Rood et al.,  
9 2010). Samples with as few as several hundred  $^{10}\text{Be}$  atoms  $\text{g}^{-1}$  quartz, the equivalent of less than  
10 100 years of surface exposure at sea level and high latitude, can now be measured above  
11 background (Corbett et al., 2015).

12

### 13 **3. Background and Study Design**

14 In 2008, a new cosmogenic extraction laboratory was built at the University of Vermont.  
15 The laboratory was designed to maximize sample throughput, minimize isobaric  $^{10}\text{B}$   
16 interference, and provide a clean workspace so as to lower  $^{10}\text{Be}/^9\text{Be}$  backgrounds. While  
17 developing the new laboratory space, we refined the sample preparation methodology that the  
18 laboratory had used for more than a decade (Hunt et al., 2008). The goal was to produce pure,  
19 high-yield samples of BeO that consistently performed similarly to standards during AMS  
20 analysis in order to maximize both accuracy and precision.

21 During the first half of 2009, we tested and refined sample processing procedures (Fig.  
22 1). We focused on three parts of the procedure: tracing beryllium through the extraction process  
23 to maximize yield, improving column performance to generate high-purity Be, and reducing

1 backgrounds to improve detection limits. From 2009-2012, five University of Vermont graduate  
2 students, three laboratory visitors, and a faculty member processed ~800 *in situ*  $^{10}\text{Be}$  samples in  
3 the new laboratory using these modified procedures and then measured the samples by AMS at  
4 Lawrence Livermore National Laboratory. Here, we use data from these ~800 samples to make  
5 inferences about the effectiveness of methodological optimization following the guidance  
6 provided by Hunt et al. (2008).

7 We use  $^9\text{Be}^{3+}$  beam currents of samples as our primary, first-order metric for quantifying  
8 sample performance during AMS analysis. For the sake of consistency between samples, which  
9 were counted between two and four separate times depending on the  $^{10}\text{Be}/^9\text{Be}$  ratio and desired  
10 precision, we report the average  $^9\text{Be}^{3+}$  beam current of the first two 300-second counting cycles  
11 of each sample. We present both measured beam currents ( $\mu\text{A}$ ) as well as normalized beam  
12 currents in order to remove run-to-run variability in AMS tuning and source performance. We  
13 normalized sample beam currents to the average beam current from the first run of all (both  
14 primary and secondary) standards on the same wheel. A normalized current of 1.0 indicates that  
15 the sample performed as well as the standards, a normalized current of less than 1.0 indicates that  
16 the sample did not perform as well as the standards, and a normalized current of greater than 1.0  
17 indicates that the sample outperformed the standards.

18 Much of our analysis and discussion focuses on cation exchange column  
19 chromatography, which removes B and Ti and separates Be from Al (Clifford, 1999; Ochs and  
20 Ivy-Ochs, 1997). The rate at which Ti, Be, and Al elute through cation exchange columns  
21 depends on multiple factors including column geometry, resin type, resin mesh size, resin bed  
22 volume, and acid strength (Clifford, 1999). In our discussion of sample purity and column  
23 chromatography, we report both the total mass of the ions of interest (in  $\mu\text{g}$ ) as well as their

1 charge equivalents (in milli-equivalents, or meq, where one meq is equal to one milli-mol of  
2 charge). For example, for Al, which forms a +3 cation and has a molar mass of  $\sim 27 \text{ g mol}^{-1}$ , 1000  
3  $\mu\text{g}$  Al is equivalent to 0.11 meq; for Ti, which forms a +4 cation but has a greater molar mass  
4 ( $\sim 48 \text{ g mol}^{-1}$ ), 1000  $\mu\text{g}$  Ti is equivalent to 0.08 meq.

## 6 **4. Methods**

### 7 *4.1. Laboratory Design and Method Development*

8 We optimized laboratory design to minimize background levels of  $^{10}\text{Be}$ . Air is supplied to  
9 the laboratory by a dedicated air handler with three filtration stages (35% and 90% boron-free  
10 polypropylene filter media, followed by diffuser-mounted Ultra Low Particle (ULPA) filters  
11 made of synthetic material). Each fully exhausting laminar flow fume hoods draws ambient air  
12 from the laboratory; this air is 35% and ULPA filtered before entering the hoods and all lab air is  
13 exhausted rather than recirculated. Although the laboratory was not built to a specific cleanroom  
14 standard, particle tests run during operation indicate that laboratory air contains about 0.2  
15 particles per cubic centimeter, consistent with a class 100 to class 1000 cleanroom. Only  
16 deionized water (17.3-17.7 Mohm) is supplied to the laboratory; before the water is used for  
17 dilution or washing, it is polished using Milli-Q deionization units equipped with boron-specific,  
18 Q-gard cartridges. We use two fully separate processing streams with dedicated labware and  
19 hood space to separate high-level samples ( $^{10}\text{Be}/^9\text{Be} > 10^{-13}$ ) from low-level samples ( $^{10}\text{Be}/^9\text{Be} <$   
20  $10^{-13}$ ).

21 We also optimized laboratory design to minimize ambient boron levels. Fiberglass  
22 insulation was replaced by foam and rock wool, and prefabricated aluminum wall panels were  
23 used in place of sheetrock. We used water leaching to test all laboratory materials and, finding

1 detectable boron in most paper and cardboard products, have minimized their use in the lab and  
2 in air filtration materials.

3 We designed the laboratory to have perchloric-acid compatible fume hoods with a  
4 washdown system. Post-dissolution high-temperature sample fuming with perchloric acid breaks  
5 down insoluble fluoride compounds and evaporates residual fluorides (Ochs and Ivy-Ochs,  
6 1997), which can negatively impact the cation column elution curve if they persist in samples.

7 To minimize acid consumption and speed throughput, we use 3 mL anion columns  
8 (Dowex 1X8 200-400 mesh resin,  $1.2 \text{ meq mL}^{-1}$ , total capacity = 3.6 meq) and 5 mL cation  
9 columns (Dowex 50WX8 200-400 mesh resin,  $1.7 \text{ meq mL}^{-1}$ , total capacity = 8.5 meq). We use  
10 double-fritted columns for both (Fig. 2); the second frit sits 1-2 mm above the resin bed and  
11 maintains a thin layer of solution between the top of the resin bed and the bottom of the second  
12 frit.

13 We repeatedly tested column performance before processing samples using quartz digests  
14 spiked with differing concentrations of additional Al and Ti. During the earlier tests, the goal  
15 was to determine the most effective way to separate the three elution peaks (Ti, Be, and Al) by  
16 experimenting with acid strength and elution volume, and collecting all of the eluted solution for  
17 Inductively-Coupled Plasma Optical Emission Spectrometry (ICP-OES) analysis (Fig. 3). To  
18 ensure that samples are Ti-free, we continue Ti elution until all Ti is removed, even if small  
19 amounts of Be (several percent of the total load) may be lost. We add hydrogen peroxide to the  
20 sample before column chromatography which stains the Ti red, providing a visual confirmation  
21 that it has been completely removed before Be elution begins (Clifford, 1999).

22 After optimizing the column elution procedure, later tests were targeted at determining  
23 the total cation load (charge equivalent) that the columns could handle by spiking quartz to



1 various impurity levels and determining the threshold of column failure. Column failure occurred  
2 when elements eluted prematurely, contaminating the Be fraction with both Ti and Al (Fig. 3). In  
3 our experiments, failure occurred at ~10% capacity, or ~0.85 meq for the cation columns. For Al  
4 (+3 charge, ~27 g mol<sup>-1</sup> molar mass), this equates to 7,650 µg; for Ti (+4 charge, ~48 g mol<sup>-1</sup>  
5 molar mass), this equates to 10,200 µg (however, actual quartz contains many different cations).

6

#### 7 *4.2. Quartz Purity and Sample Massing*

8         Rock samples are crushed, ground, and sieved, while sediment samples are just sieved.  
9 To isolate quartz from other mineral phases, we use magnetic separation, repeated acid etches,  
10 and density separation if necessary (Kohl and Nishiizumi, 1992). After etching, 0.25 g aliquots  
11 of purified quartz are dissolved in concentrated HF and tested for purity with regard to major  
12 elements (Al, Ca, Fe, K, Mg, Na, and Ti) using a rapid ICP-OES method. Quartz with high  
13 impurity levels is re-etched for an additional week, then tested again.

14         We use quartz cation concentrations to decide how much sample can be dissolved  
15 without overloading the ion exchange columns. Because our experimentation has shown that  
16 cation column failure occurs at ~10% of the total resin capacity, we limit the amount of quartz  
17 we dissolve based on its purity such that we load only ~0.85 meq to our 5 mL cation columns.  
18 This is a conservative approach because perchloric acid treatments oxidize much of the Ti (Hunt  
19 et al., 2008), which is later removed by centrifugation. We use up to ~20 g of quartz for high-  
20 level samples (<sup>10</sup>Be/<sup>9</sup>Be > 10<sup>-13</sup>) and up to ~40 g of quartz for low-level samples (<sup>10</sup>Be/<sup>9</sup>Be < 10<sup>-</sup>  
21 <sup>13</sup>); these upper limits for quartz mass were chosen based on the capacity of the Teflon labware  
22 we use for dissolution and extraction.

1 To the quartz, we add 250  $\mu\text{g}$   $^9\text{Be}$  via in-house made beryl-derived carrier solution.  
2 Additions of  $^{27}\text{Al}$  (via SPEX Al standard) are determined based on the quantified native Al in the  
3 quartz, with the aim of having  $\sim 2000$   $\mu\text{g}$  Al in each sample. We digest samples in HF ( $\sim 5$  g HF  
4 per g quartz) over several days, increasing the digest temperature incrementally up to  $135^\circ\text{C}$ .

5

#### 6 *4.3. Blanks*

7 Each batch of ten samples includes one blank and one CRONUS standard for high-level  
8 samples ( $^{10}\text{Be}/^9\text{Be} > 10^{-13}$ ) and two blanks for low-level samples ( $^{10}\text{Be}/^9\text{Be} < 10^{-13}$ ). We currently  
9 use  $^9\text{Be}$  carrier made in-house by the flux fusion of beryl (Stone, 1998) for all samples; however,  
10 the earliest high-level samples had blanks of SPEX brand 1000 ppm ICP elemental standard. All  
11 of these process blanks as well as samples contain  $\sim 250$   $\mu\text{g}$   $^9\text{Be}$ .

12

#### 13 *4.4. Post-Dissolution Aliquots*

14 Immediately following dissolution, we remove replicate aliquots directly from the HF  
15 digestion solution, quantifying the percentage of solution removed by mass. These aliquots  
16 represent  $\sim 2\%$  and  $4\%$  of the total sample mass, respectively. To each aliquot we add a small  
17 amount of  $\text{H}_2\text{SO}_4$  to ensure the aliquot does not reach dryness, evaporate the HF, and then add  
18 (by mass) a  $1\%$   $\text{H}_2\text{SO}_4$  solution spiked with Ga and Y to act as an internal standards and correct  
19 for instrument drift. We use these aliquots to quantify Be and Al at high precision (percent level)  
20 with ICP-OES, using multiple measurement lines for each element (Be, 234.861 and 249.473  
21 nm; and Al, 308.215 and 309.271 nm).

22

23

1 *4.5. Be Isolation and Post-Processing Aliquots*

2           Following removal of post-dissolution aliquots, we evaporate the remaining HF and fume  
3 the samples three separate times with perchloric acid at 230°C to break up and drive off fluoride  
4 compounds (Ochs and Ivy-Ochs, 1997). We then centrifuge samples to remove Ti and insoluble  
5 fluorides, convert samples to chloride form by fuming with and dissolving in HCl, and perform  
6 anion column chromatography to remove Fe. After anion column chromatography, we evaporate  
7 the HCl, convert samples to sulfate form, and perform cation column chromatography to remove  
8 B and Ti and separate Be from Al (Clifford, 1999; Ochs and Ivy-Ochs, 1997).

9           At the end of the extraction process and before hydroxide precipitation, we test the Be  
10 fraction for yield and purity by extracting small aliquots. Because we employ a volumetric  
11 dilution and a rapid ICP-OES method to speed the process, the precision of these data is less than  
12 that of the post-dissolution aliquots. Samples are then precipitated as Be hydroxide at pH ~8  
13 (using methyl red, a liquid pH indicator), dried, converted to BeO using an air/wall gas flame,  
14 combined with Nb at a 1:1 molar ratio (Hunt et al., 2006), and packed into stainless steel  
15 cathodes for AMS analysis.

16

17 **5. Results**

18 *5.1. Quartz Purity*

19           Quartz purity varies appreciably between study sites. Of the 797 quartz samples tested  
20 during 2009-2012, the average total cation concentration was  $333 \pm 359 \mu\text{g g}^{-1}$  (1SD) in terms of  
21 mass, or  $0.024 \pm 0.038 \text{ meq g}^{-1}$  (1SD) in terms of charge (Fig. 4). On average, almost half of this  
22 concentration is comprised of Al ( $119 \pm 117 \mu\text{g g}^{-1}$ , or  $0.013 \pm 0.013 \text{ meq g}^{-1}$ , 1SD, Fig. 4).

1 However, since Fe is removed during anion column chromatography, the effective total load  
2 during cation chromatography excludes Fe and averages  $272 \mu\text{g g}^{-1}$  ( $0.021 \text{ meq g}^{-1}$ ).

3

#### 4 *5.2. Post-Dissolution Aliquots*

5 Because samples have only been dissolved at the point we remove these aliquots and  
6 there is no mechanism for Be loss, post-dissolution aliquots should return 100% of the Be that  
7 was added to the sample through  $^9\text{Be}$  carrier (plus any native  $^9\text{Be}$  contained within the quartz).

8 Aliquot measurements of blanks yielded  $100.7 \pm 2.1 \%$  (mean,  $n = 114$ , 1SD) of the  
9 expected Be based on the mass and concentration of  $^9\text{Be}$  carrier added (Fig. 5a). This value  
10 suggests that our ICP-OES precision for Be measurements in this context is  $\sim 2\%$  (1SD), which is  
11 greater than the uncertainty of individual ICP replicates (usually  $\leq 1\%$ ) but similar to nominal  
12 precision of many AMS  $^{10}\text{Be}$  analyses at present (Rood et al., 2013). Aliquot measurements of  
13 blanks are normally-distributed.

14 Aliquot measurements of samples are more variable than those of the blanks and have a  
15 long-tailed distribution skewed toward higher values. Quantification of Be in samples yielded an  
16 average of  $100.8 \pm 22.4 \%$  (mean,  $n = 797$ , 1SD) of the expected Be based on the mass and  
17 concentration of  $^9\text{Be}$  carrier added (Fig. 5b).

18

#### 19 *5.3. Post-Processing Aliquots*

20 For the post-processing aliquots, Be yield should be 94% because 6% of the total sample  
21 is removed for the post-dissolution aliquots. For the process blanks, the measured Be yield is  
22  $94.0 \pm 3.6 \%$  (mean,  $n = 114$ , 1SD, Fig. 6a) of the total Be based on the mass and concentration  
23 of  $^9\text{Be}$  carrier added. For samples, the measured Be yield is  $93.9 \pm 21.6 \%$  (mean,  $n = 797$ , 1SD,

1 Fig. 6b) of the total. When considered in reference to the quartz that was dissolved, laboratory  
2 treatment of Be fractions decreased average total sample Al contents by 99.1%, Fe contents by  
3 99.5%, and Ti contents by 99.9% (n = 797, Fig. 7).

#### 5 *5.4. Background $^{10}\text{Be}/^9\text{Be}$ Ratios*

6 Measured isotopic ratios of process blanks reflect the type of carrier used in their  
7 preparation and the average  $^{10}\text{Be}$  concentration of samples processed in the batches  
8 accompanying the blanks. Beryl blanks are lower ( $5.6 \pm 3.2 \times 10^{-16}$ , 1SD, n = 59) in the hood  
9 used to process low-level samples and higher ( $9.0 \pm 8.9 \times 10^{-16}$ , 1SD, n = 29) in the hood used to  
10 process high-level samples (Fig. 8). When assessed in an unequal variance Student's T-Test,  
11 beryl blank ratios between the two hoods are statistically separable (p = 0.004). SPEX carrier  
12 blanks in the high-level hood have an average ratio more than an order of magnitude higher than  
13 beryl blanks in the same hood ( $1.2 \pm 0.1 \times 10^{-14}$ , 1SD, n = 19, Fig. 8). When assessed in an  
14 unequal variance Student's T-Test, the ratios of the SPEX blanks and the beryl blanks processed  
15 in the same hood are statistically separable (p < 0.001).

16 For beryl blanks processed in the low-level hood, the standard deviation of the 59  
17 different measurements (57%) is larger than the average measurement uncertainty (36%). For  
18 beryl blanks processed in the high-level hood, the discrepancy between the standard deviation of  
19 the 29 measurements (82%) and the average measurement uncertainty (29%) is greater. For  
20 SPEX blanks processed in the high-level hood, the standard deviation of the 19 measurements  
21 (4%) is less than the average measurement uncertainty (7%), although both values are  
22 appreciably smaller than for beryl blanks because there are more  $^{10}\text{Be}$  counts resulting in more  
23 precise data. Over time (2009-2012), there appears to be no trend in process blank  $^{10}\text{Be}/^9\text{Be}$

1 ratios (Fig. 9).

2

### 3 *5.5. Sample Beam Currents*

4 The AMS  $^9\text{Be}^{3+}$  beam currents of samples were consistent for samples processed during  
5 2009-2012 (Fig. 10). The average beam current for samples was  $21.4 \pm 3.8 \mu\text{A}$  (1 SD,  $n = 797$ ).

6 The beam current normalized to standards run with these samples averaged  $1.0 \pm 0.2$  (1 SD,  $n =$   
7 797). Quartz purity (expressed as total cation load) is not significantly related to normalized  
8 sample  $^9\text{Be}^{3+}$  beam current ( $R^2 = 0.004$ ,  $p = 0.066$ ) indicating that our optimized laboratory  
9 methods are able to compensate for a wide range of initial quartz impurity concentrations.

10 Analysis of  $^9\text{Be}^{3+}$  beam currents also indicates that the methods we describe here yield  
11 more predictable sample performance than those used previously in the University of Vermont  
12 cosmogenic nuclide laboratory. A previous assessment of data quality by Hunt et al. (2008)  
13 showed a greater range of beam currents, yielding a relative standard deviation of  $\sim 40\%$  ( $n = 63$ ).  
14 The beam current data we show here have a relative standard deviation of 18% ( $n = 797$ ).

15

## 16 **6. Discussion**

### 17 *6.1. Tracing Beryllium Through the Extraction Process*

18 Tracing Be throughout the extraction process provides insight about the samples at two  
19 steps. Analysis of post-dissolution aliquots (Fig. 5) quantifies if any native  $^9\text{Be}$  is present in the  
20 quartz (Portenga et al., 2015), while analysis of post-processing aliquots (Fig. 6) serves as a  
21 quality control metric to assess final Be yield and ensure that all samples have consistent Be  
22 mass (Hunt et al., 2008). Rare departures from the expected values for these two parameters may

1 indicate the need for corrections, either accounting for native  $^9\text{Be}$  in the data reduction or  
2 identifying and remediating sources of Be loss.

3 For the post-dissolution aliquots (Fig. 5), which should return 100% of the expected Be  
4 based on carrier addition, the few samples more than 2% (the 1SD precision of our analyses  
5 based on the performance of the blanks) below the central tendency likely reflect massing errors  
6 or ICP-OES interferences from rare accessory elements in quartz. Samples more than 2% (1SD,  
7 based on analysis of blanks) above the central tendency are those in which the quartz likely  
8 contained native  $^9\text{Be}$ . For the post-processing aliquots (Fig 6), which should return 94% Be yield,  
9 samples considerably below 94% may be a result of laboratory error (for example, spilling a  
10 sample) and/or limitations during measurement such as interfering peaks. Samples falling  
11 considerably above 94% Be yield likely indicate the presence of  $^9\text{Be}$  in quartz, which can be  
12 verified by cross-checking against the higher-precision post-dissolution aliquot measurements.

13 Be tracing unambiguously demonstrates the presence of native  $^9\text{Be}$  in some purified  
14 quartz mineral separates (Figs. 5b and 6b) and allows the mass of native  $^9\text{Be}$  to be incorporated  
15 in the calculation of  $^{10}\text{Be}$  concentrations derived from the measured  $^{10}\text{Be}/^9\text{Be}$  ratio. Although our  
16 ability to detect small amounts (few  $\mu\text{g}$ ) of native Be is limited by the overall precision of ICP-  
17 OES analysis ( $\sim 2\%$  for the post-dissolution aliquots, as described above), such small additions of  
18 native Be are less important as they do not change calculated  $^{10}\text{Be}$  concentrations beyond the  
19 precision of the AMS measurements. Because the method we use can reliably detect larger  
20 amounts ( $> 10 \mu\text{g}$ ) of native Be, an amount which begins to impact the resulting data at the  
21 several percent level, we can correct for its presence. Considering the dataset assessed here (Fig.  
22 5b), 56 of the 797 samples (or  $\sim 7\%$  of the population) exceed the expected Be measurement by 2

1 SD (4%) and 38 of the 797 samples (or ~5% of the population) exceed the expected Be  
2 measurement by 3 SD (6%).

3 Failing to identify and correct for native Be in those samples for which quartz contributes  
4 more than a few  $\mu\text{g}$  of Be will cause errors in the calculation of  $^{10}\text{Be}$  concentration and thus in  
5 the inferred erosion rates, exposure ages, and dual isotope ratios. For example, in a suite of 49  
6 samples from Bhutan prepared at University of Vermont, most samples contained detectable  
7 native  $^9\text{Be}$  (Portenga et al., 2015). Approximately 240  $\mu\text{g}$  of  $^9\text{Be}$  carrier was added to each of the  
8 Bhutan samples as a spike; however, ICP-OES analysis of aliquots demonstrated that samples  
9 contained 244-1158  $\mu\text{g}$  total  $^9\text{Be}$ , indicating native  $^9\text{Be}$  loads of as much as 900  $\mu\text{g}$  per sample  
10 and native  $^9\text{Be}$  concentrations in quartz as high as 38  $\mu\text{g g}^{-1}$  (see Figure 3 in Portenga et al.  
11 (2015)). These native  $^9\text{Be}$  concentrations are as much as 4-5 times greater than the amount of  $^9\text{Be}$   
12 carrier added. The source of this native Be may include beryl crystals, fluid inclusions in quartz  
13 grains, and/or structural substitution in quartz grains (Grew, 2002). Failure to detect and correct  
14 for this native  $^9\text{Be}$  would have caused erosion rate overestimates of as much as 400% (Portenga  
15 et al., 2015).

16 Post-processing aliquots (Fig. 6) serve as a quality check at the end of the extraction  
17 procedure to verify that samples are ready for AMS analysis and provides quality control in a  
18 laboratory where many different people each year are preparing samples. Quantifying the Be  
19 yield determines if enough Be is present for a successful AMS measurement. If sufficient Be is  
20 not present in the sample, the Ti fraction is analyzed by ICP-OES; in this case (which has  
21 happened only once when elution acid was incorrectly mixed), the missing Be eluted through the  
22 cation column early and was recovered by reprocessing the Ti fraction.

23



## 1 6.2. Producing Pure Beryllium

2 Creation of high-purity Be fractions ensures that samples will perform similarly to the  
3 standards during AMS analysis and provides a constant mass of material to load into cathodes.  
4 We demonstrate here that Be purity can be maximized by improving and calibrating/verifying  
5 column chromatography methods, tailoring the mass of quartz so as not to overload the columns,  
6 and verifying purity via quality control post-processing aliquots (Fig. 7). Constant  $^9\text{Be}$  mass  
7 results in a uniform depth to the material surface and a consistent mixing ratio with Nb, which  
8 optimizes the ionization yield, the AMS sputtering efficiency, and the measurement  
9 reproducibility (Rood et al., 2010) for sputter sources using front-loaded cathodes.

10 Optimized column methodology improves data quality and reduces the time needed to  
11 make AMS measurements. After cation column chromatography, post-processing aliquots show  
12 that Be fractions are consistently free of impurities (Fig. 7), contain virtually all of the original  
13 Be (Fig. 6), and that the resulting  $^9\text{Be}^{3+}$  beam current is not related to the purity of the quartz.  
14 Even in small concentrations, Ti is thought to diminish  $^9\text{Be}^{3+}$  beam currents beyond the dilution  
15 effects (Hunt et al., 2008). If Al, Fe, or Ti are present at greater than trace levels ( $>100\ \mu\text{g}$  for Al,  
16 Fe, and Ti) in the post-column Be fraction, which occurs only rarely, the Be fraction can be  
17 neutralized, precipitated, re-dissolved, and cycled through anion and/or cation columns a second  
18 time to remove remaining impurities. We are unable to definitively address the impact of Ti on  
19  $^9\text{Be}^{3+}$  beam currents with our dataset since we have successfully removed Ti from the samples  
20 described here (Fig. 7) and hence do not have a range of Ti values over which to assess resulting  
21 beam currents.

22 The double-fritted column configuration (Fig. 2) has several benefits. The second frit  
23 prevents the column from drying out during the elution process, thereby avoiding channeling

1 which can allow solution to bypass the resin. In addition, the second frit ensures that the resin  
2 bed is not disturbed while adding solutions, allowing the column steps to be performed in a more  
3 time-efficient and reproducible manner; cation column chromatography on a batch of 12 samples  
4 can be performed in 3-4 hours. These double-fritted columns have successfully been regenerated  
5 and re-used for several years (more than 50 batches of samples) by stripping them with acid,  
6 flushing them with water, and storing them fully saturated in water between uses. Over that time,  
7 there has been no change in column performance or blank values.

8

### 9 *6.3. Reducing Backgrounds to Improve Detection Limits*

10 Backgrounds are an important control on the accuracy and precision of  $^{10}\text{Be}$  analyses,  
11 especially for samples with low  $^{10}\text{Be}/^9\text{Be}$  ratios. Improved AMS techniques now consistently  
12 produce machine blanks with  $^{10}\text{Be}/^9\text{Be}$  ratios well below  $10^{-15}$  (Rood et al., 2010), placing  
13 greater demands on processing laboratories to both minimize sample cross-talk and lower the  
14 amount of the interfering isobar,  $^{10}\text{B}$ .

15 Using beryl carrier and processing low-level samples in a separate fully-exhausting  
16 laminar flow hood with dedicated labware resulted in blanks almost two orders of magnitude  
17 lower than using commercial carrier (Figs. 8 and 9). The methodology described here routinely  
18 achieves blanks with  $^{10}\text{Be}/^9\text{Be}$  ratios in the mid  $10^{-16}$  level, allowing samples with ratios in the  
19 low  $10^{-15}$  level to be measured. Decreasing the detection limits of  $^{10}\text{Be}$  analysis by AMS opens  
20 new frontiers for the types of samples that can be studied. In particular, having lower detection  
21 limits enables the analysis of samples with little  $^{10}\text{Be}$ , including those that are very young  
22 (Licciardi et al., 2009), those that have been subjected to rapid erosion (Portenga et al., 2015), or  
23 those that have been buried for long durations (Erlanger et al., 2012; Gibbon et al., 2014).

1 **7. Conclusions**

2 Analysis of quality control data associated with ~800  $^{10}\text{Be}$  samples prepared at the  
3 University of Vermont and measured at Lawrence Livermore National Laboratory shows that  
4 methodological optimization can yield samples that perform consistently and similarly to  
5 standards during AMS analysis. While data accuracy and precision are, to some extent,  
6 controlled by design, performance, and operation of the AMS, both are also influenced by the  
7 chemistry and sample preparation performed by cosmogenic extraction laboratories. We  
8 demonstrate that methodological optimization aimed at maximizing Be yield, while minimizing  
9 contaminants and background levels of  $^{10}\text{Be}$  and  $^{10}\text{B}$ , can increase data accuracy and precision  
10 and lower detection limits (although replicate analyses of internal geologic standards could  
11 further assess accuracy and precision of the chemical methods we employ here). Methodological  
12 optimization also helps to identify and address problematic samples, such as those containing  
13 native Be or high concentrations of accessory cations, and improves time efficiency of laboratory  
14 methods and AMS analysis. Such enhancements in data quality and efficiency can open new  
15 frontiers for the scientific questions that can be addressed with *in situ* produced  $^{10}\text{Be}$ .

16

17 **Acknowledgements**

18 Method development and sample analyses described here were supported by the National  
19 Science Foundation (especially ARC-1023191 and ARC-0713956 to Bierman and EAR-0948350  
20 to Rood) and the University of Vermont. Corbett was supported by a National Science  
21 Foundation Graduate Research Fellowship and a Doctoral Dissertation Research Improvement  
22 Grant (BCS-1433878). We thank the staff of CAMS-LLNL for assistance in making  $^{10}\text{Be}$   
23 measurements and two anonymous reviewers for improving the manuscript.

## References

- Balco, G., 2011. Contributions and unrealized potential contributions of cosmogenic-nuclide exposure dating to glacier chronology, 1990-2010. *Quaternary Science Reviews* 30, 3-27.
- Balco, G., Briner, J., Finkel, R., Rayburn, J., Ridge, J., Schaefer, J., 2009. Regional beryllium-10 production rate calibration for late-glacial northeastern North America. *Quaternary Geochronology* 4, 93-107.
- Balco, G., Rovey, C., 2008. An isochron method for cosmogenic-nuclide dating of buried soils and sediments. *American Journal of Science* 308, 1083-1114.
- Balco, G., Stone, J., Lifton, N., Dunai, T., 2008. A complete and easily accessible means of calculating surface exposure ages or erosion rates from  $^{10}\text{Be}$  and  $^{26}\text{Al}$  measurements. *Quaternary Geochronology* 3, 174-195.
- Bierman, P., Gillespie, A., Caffee, M., 1995. Cosmogenic ages for earthquake recurrence intervals and debris flow fan deposition, Owens Valley, California. *Science* 270, 447-450.
- Bierman, P., Marsella, K., Patterson, C., Davis, P., Caffee, M., 1999. Mid-Pleistocene cosmogenic minimum-age limits for pre-Wisconsinan glacial surfaces in southwestern Minnesota and southern Baffin Island: a multiple nuclide approach. *Geomorphology* 27, 25-39.
- Bierman, P., Nichols, K., 2004. Rock to sediment- slope to sea with  $^{10}\text{Be}$ - rates of landscape change. *Annual Review of Earth and Planetary Sciences* 32, 215-255.
- Bierman, P., Steig, E., 1996. Estimating rates of denudation using cosmogenic isotope abundances in sediment. *Earth Surface Processes and Landforms* 21, 125-139.
- Borchers, B., Marrero, S., Balco, G., Caffee, M., Goehring, B., Lifton, N., Nishiizumi, K., Phillips, F., Schaefer, J., Stone, J., 2015. Geological calibration of spallation production rates in the CRONUS-Earth project. *Quaternary Geochronology* doi:10.1016/j.quageo.2015.01.009.
- Briner, J., Young, N., Goehring, B., Schaefer, J., 2012. Constraining Holocene  $^{10}\text{Be}$  production rates in Greenland. *Journal of Quaternary Science* 27, 2-6.
- Brown, E., Bourles, D., Raisbeck, G., Yiou, F., Burchfiel, B., Molnar, P., Qidong, D., Jun, L., 1998. Estimation of slip rates in the southern Tien Shan using cosmic ray exposure dates of abandoned alluvial fans. *Geological Society of America Bulletin* 110, 377-386.
- Brown, E., Edmond, J., Raisbeck, G., Yiou, F., Kurz, M., Brook, E., 1991. Examination of surface exposure ages of Antarctic moraines using in situ produced  $^{10}\text{Be}$  and  $^{26}\text{Al}$ . *Geochimica et Cosmochimica Acta* 55, 2269-2283.
- Brown, E., Stallard, R., Larsen, M., Raisbeck, G., Yiou, F., 1995. Denudation rates determined from the accumulation of in situ-produced  $^{10}\text{Be}$  in the Luquillo Experimental Forest, Puerto Rico. *Earth and Planetary Science Letters* 129, 193-202.
- Chmeleff, J., Von Blanckenburg, F., Kossert, K., Jakob, D., 2010. Determination of the  $^{10}\text{Be}$  half-life by multicollector ICP-MS and liquid scintillation counting. *Nuclear Instruments and Methods in Physics Research Section B: Beam Interactions with Materials and Atoms* 268, 192-199.
- Clifford, D., 1999. Ion-exchange and inorganic adsorption, *Water Quality and Treatment: A Handbook of Community Water Supplies*. American Water Works Association, McGraw-Hill, New York.

- Corbett, L., Bierman, P., Neumann, T., Graly, J., 2015. Inferring glacial history and subglacial process through analysis of cosmogenic nuclides in icebound cobbles. American Geophysical Union Fall Meeting Abstract ID C11A-0745.
- Ditchburn, R., Whitehead, N., 1994. The separation of  $^{10}\text{Be}$  from silicates, 3rd Workshop of the South Pacific Environmental Radioactivity Association, pp. 4-7.
- Erlanger, E., Granger, D., Gibbon, R., 2012. Rock uplift rates in South Africa from isochron burial dating of fluvial and marine terraces. *Geology* 40, 1019-1022.
- Fabel, D., Harbor, J., 1999. The use of in-situ produced cosmogenic radionuclides in glaciology and glacial geomorphology. *Annals of Glaciology* 28, 103-110.
- Fairhall, A., 1960. The Radiochemistry of Beryllium, Nuclear Science Series. National Academy of Sciences and National Research Council, Washington, DC.
- Gibbon, R., Pickering, T., Sutton, M., Heaton, J., Kuman, K., Clarke, R., Brain, C., Granger, D., 2014. Cosmogenic nuclide burial dating of hominin-bearing Pleistocene cave deposits at Swartkrans, South Africa. *Quaternary Geochronology* 24, 10-15.
- Gosse, J., Phillips, F., 2001. Terrestrial in situ cosmogenic nuclides: theory and application. *Quaternary Science Reviews* 20, 1475-1560.
- Granger, D., Kirchner, J., Finkel, R., 1996. Spatially averaged long-term erosion rates measured from in situ-produced cosmogenic nuclides in alluvial sediment. *The Journal of Geology* 104, 249-257.
- Granger, D., Lifton, N., Willenbring, J., 2013. A cosmic trip: 25 years of cosmogenic nuclides in geology. *Geological Society of America Bulletin* 125, 1379-1402.
- Granger, D., Muzikar, P., 2001. Dating sediment burial with in situ-produced cosmogenic nuclides: theory, techniques, and limitations. *Earth and Planetary Science Letters* 188, 269-281.
- Grew, E., 2002. Beryllium in metamorphic environments (emphasis on aluminous compositions), in: Grew, E. (Ed.), Volume 50: Beryllium: Mineralogy, Petrology, and Geochemistry. Mineralogical Society of America, Chantilly, Virginia, p. 690.
- Heyman, J., Stroeven, A., Harbor, J., Caffee, M., 2011. Too young or too old: Evaluating cosmogenic exposure dating based on an analysis of compiled boulder exposure ages. *Earth and Planetary Science Letters* 302, 71-80.
- Hunt, A., Larsen, J., Bierman, P., Petrucci, G., 2008. Investigation of factors that affect the sensitivity of accelerator mass spectrometry for cosmogenic  $^{10}\text{Be}$  and  $^{26}\text{Al}$  isotope analysis. *Analytical Chemistry* 80, 1656-1663.
- Hunt, A., Petrucci, G., Bierman, P., Finkel, R., 2006. Metal matrices to optimize ion beam currents for accelerator mass spectrometry. *Nuclear Instruments and Methods in Physics Research Section B: Beam Interactions with Materials and Atoms* 243, 216-222.
- Hunt, A., Petrucci, G., Bierman, P., Finkel, R., 2007. Investigation of metal matrix systems for cosmogenic  $^{26}\text{Al}$  analysis by accelerator mass spectrometry. *Nuclear Instruments and Methods in Physics Research B* 260, 633-636.
- Klein, J., Middleton, R., 1984. Accelerator mass spectrometry at the University of Pennsylvania. *Nuclear Instruments and Methods in Physics Research Section B: Beam Interactions with Materials and Atoms* 5, 129-133.
- Kohl, C., Nishiizumi, K., 1992. Chemical isolation of quartz for measurement of in-situ-produced cosmogenic nuclides. *Geochimica et Cosmochimica Acta* 56, 3583-3587.
- Korschinek, G., Bergmaier, A., Faestermann, T., Gerstmann, U., Knie, K., Rugel, G., Wallner, A., Dillmann, I., Dollinger, G., Lierse von Gostomski, C., Kossert, K., Maiti, M.,

- Poutivtsev, M., Remmert, A., 2010. A new value for the half-life of  $^{10}\text{Be}$  by Heavy-Ion Elastic Recoil Detection and liquid scintillation counting. *Nuclear Instruments and Methods in Physics Research Section B: Beam Interactions with Materials and Atoms* 268, 187-191.
- Lal, D., 1988. In situ-produced cosmogenic isotopes in terrestrial rocks. *Annual Review of Earth and Planetary Sciences* 16, 355-388.
- Lanford, W., Parker, P., Bauer, K., Turekian, K., Cochran, J., Krishnaswami, S., 1980. Measurements of  $^{10}\text{Be}$  distributions using a Tandem Van De Graaff accelerator. *Nuclear Instruments and Methods* 168, 505-510.
- Licciardi, J., Schaefer, J., Taggart, J., Lund, D., 2009. Holocene glacier fluctuations in the Peruvian Andes indicate northern climate linkages. *Science* 325, 1677-1679.
- Matmon, A., Schwartz, D., Finkel, R., Clemmens, S., Hanks, T., 2005. Dating offset fans along the Mojave section of the San Andreas fault using cosmogenic  $^{26}\text{Al}$  and  $^{10}\text{Be}$ . *Geological Society of America Bulletin* 117, 795-807.
- Merchel, S., Arnold, M., Aumaitre, G., Benedetti, L., Bourles, D., Braucher, R., Alfimov, V., Freeman, S., Steier, P., Wallner, A., 2008. Towards more precise  $^{10}\text{Be}$  and  $^{36}\text{Cl}$  data from measurements at the  $10^{-14}$  level: Influence of sample preparation. *Nuclear Instruments and Methods in Physics Research Section B: Beam Interactions with Materials and Atoms* 266, 4921-4926.
- Merchel, S., Bremser, W., Akhmadaliev, S., Arnold, M., Aumaitre, G., Bourles, D., Braucher, R., Caffee, M., Christl, M., Fifield, K., Finkel, R., Freeman, S., Ruiz-Gomez, A., Kubik, P., Martschini, M., Rood, D., Tims, S., Wallner, A., Wilcken, K., Xu, S., 2012. Quality assurance in accelerator mass spectrometry: Results from an international round-robin exercise for  $^{10}\text{Be}$ . *Nuclear Instruments and Methods Section B: Beam Interactions with Materials and Atoms* 289, 68-73.
- Middleton, R., Klein, J., Dezfouly-Arjomandy, B., Albrecht, A., Xue, S., Herzog, G., 1994.  $^{10}\text{Be}$  in bauxite and commercial aluminum. *Nuclear Instruments and Methods in Physics Research Section B: Beam Interactions with Materials and Atoms* 92, 362-366.
- Muzikar, P., Elmore, D., Granger, D., 2003. Accelerator mass spectrometry in geologic research. *Geological Society of America Bulletin* 115, 643-654.
- Nishiizumi, K., Imamura, M., Caffee, M., Southon, J., Finkel, R., McAninch, J., 2007. Absolute calibration of  $^{10}\text{Be}$  AMS standards. *Nuclear Instruments and Methods in Physics Research Section B: Beam Interactions with Materials and Atoms* 258, 403-413.
- Nishiizumi, K., Kohl, C., Arnold, J., Dorn, R., Klein, I., Fink, D., Middleton, R., Lal, D., 1993. Role of in situ cosmogenic nuclides  $^{10}\text{Be}$  and  $^{26}\text{Al}$  in the study of diverse geomorphic processes. *Earth Surface Processes and Landforms* 18, 407-425.
- Nishiizumi, K., Kohl, C., Arnold, J., Klein, J., Fink, D., Middleton, R., 1991. Cosmic ray produced  $^{10}\text{Be}$  and  $^{26}\text{Al}$  in Antarctic rocks: exposure and erosion history. *Earth and Planetary Science Letters* 104, 440-454.
- Nishiizumi, K., Lal, D., Klein, J., Middleton, R., Arnold, J., 1986. Production of  $^{10}\text{Be}$  and  $^{26}\text{Al}$  by cosmic rays in terrestrial quartz in situ and implications for erosion rates. *Nature* 319, 134-136.
- Nishiizumi, K., Winterer, E., Kohl, C., Klein, J., Middleton, R., Lal, D., Arnold, J., 1989. Cosmic ray production rates of  $^{10}\text{Be}$  and  $^{26}\text{Al}$  in quartz from glacially polished rocks. *Journal of Geophysical Research* 94, 17907.

- Ochs, M., Ivy-Ochs, S., 1997. The chemical behavior of Be, Al, Fe, Ca and Mg during AMS target preparation from terrestrial silicates modeled with chemical speciation calculations. *Nuclear Instruments and Methods in Physics Research B* 123, 235-240.
- Phillips, F., Zreda, M., Smith, S., Elmore, D., Kubik, P., Sharma, P., 1990. Cosmogenic chlorine-36 chronology for glacial deposits at Bloody Canyon, eastern Sierra Nevada. *Science* 248, 1529-1532.
- Portenga, E., Bierman, P., 2011. Understanding Earth's eroding surface with  $^{10}\text{Be}$ . *GSA Today* 21, 4-10.
- Portenga, E., Bierman, P., Duncan, C., Corbett, L., Kehrwald, N., Rood, D., 2015. Erosion rates of the Bhutanese Himalaya determined using in situ-produced  $^{10}\text{Be}$ . *Geomorphology* 233, 112-126.
- Putnam, A., Schaefer, J., Barrell, D., Vandergoes, M., Denton, G., Kaplan, M., Finkel, R., Schwartz, R., Goehring, B., Kelley, S., 2010. In situ cosmogenic  $^{10}\text{Be}$  production-rate calibration from the Southern Alps, New Zealand. *Quaternary Geochronology* 5, 392-409.
- Raisbeck, G., Yiou, F., Bourles, D., Ledringuez, J., Deboffe, D., 1987. Measurements of  $^{10}\text{Be}$  and  $^{26}\text{Al}$  with a tandem AMS facility. *Nuclear Instruments and Methods in Physics Research Section B: Beam Interactions with Materials and Atoms* 29, 22-26.
- Raisbeck, G., Yiou, F., Fruneau, M., Loiseaux, J., 1978. Beryllium-10 mass spectrometry with a cyclotron. *Science* 202, 215-217.
- Rood, D., Brown, T., Finkel, R., Guilderson, T., 2013. Poisson and non-Poisson uncertainty estimations of  $^{10}\text{Be}/^9\text{Be}$  measurements at LLNL-CAMS. *Nuclear Instruments and Methods in Physics Research B* 294, 426-429.
- Rood, D., Hall, S., Guilderson, T., Finkel, R., Brown, T., 2010. Challenges and opportunities in high-precision Be-10 measurements at CAMS. *Nuclear Instruments and Methods in Physics Research Section B: Beam Interactions with Materials and Atoms* 268, 730-732.
- Rood, D., Xu, S., Shank, R., Dougans, A., Gallacher, P., Keefe, K., Miguens-Rodriguez, M., Bierman, P., Carlson, A., Freeman, S., 2014. Towards high precision and low ratio Be-10 measurements with the SUERC 5MV tandem: bigger isn't always better. *The Thirteenth International Conference on Accelerator Mass Spectrometry Programme and Abstracts*, 53.
- Shanks, R., Freeman, S., 2015. Sputter-pits casting to measure AMS sample consumption. *Nuclear Instruments and Methods Section B: Beam Interactions with Materials and Atoms* 361, 168-172.
- Southon, J., Vogel, J., Nowikow, I., Nelson, D., Korteling, R., Ku, T., Kusakabe, M., Huh, C., 1983. The measurement of  $^{10}\text{Be}$  concentrations with a tandem accelerator. *Nuclear Instruments and Methods in Physics Research* 205, 251-257.
- Stone, J., 1998. A rapid fusion method for separation of beryllium-10 from soils and silicates. *Geochimica et Cosmochimica Acta* 62, 555-561.
- Suter, M., 1990. Accelerator mass spectrometry: state of the art in 1990. *Nuclear Instruments and Methods in Physics Research Section B: Beam Interactions with Materials and Atoms* 52, 211-223.
- Tera, F., Brown, L., Morris, J., Sacks, S., 1986. Sediment incorporation in island-arc magmas: Inferences from  $^{10}\text{Be}$ . *Geochimica et Cosmochimica Acta* 50, 535-550.

- Thomas, J., Manglani, A., Parker, P., 1981. Improvements in an Accelerator Based Mass Spectrometer for Measuring  $^{10}\text{Be}$ . *IEEE Transactions on Nuclear Science* 28, 1478-1480.
- Tuniz, C., Bird, J., Fink, D., Herzog, G., 1998. *Accelerator Mass Spectrometry: Ultrasensitive Analysis for Global Science*. CRC Press, Boston.
- Turekian, K., Cochran, J., Krishnaswami, S., Lanford, W., Parker, P., Bauer, K., 1979. The measurement of  $^{10}\text{Be}$  in manganese nodules using a tandem Van De Graaff accelerator. *Geophysical Research Letters* 6, 417-420.
- von Blanckenburg, F., 2005. The control mechanisms of erosion and weathering at basin scale from cosmogenic nuclides in river sediment. *Earth and Planetary Science Letters* 237, 462-479.
- von Blanckenburg, F., Willenbring, J., 2014. Cosmogenic nuclides: dates and rates of Earth-surface change. *Elements* 10, 341-346.



## Figure Legends

**Figure 1.** Flow chart of Be isotopic sample preparation. Arrows designate the direction of sample progression through the process, and gray font indicates sample fractions removed from the flow.

**Figure 2.** Diagram of a double-fritted column implemented for both anion and cation chromatography methods.

**Figure 3.** Cation chromatograms from tests performed during method development. Ti, Be, and Al are shown in light gray, medium gray, and dark gray, respectively. Top panel shows an optimized elution curve that cleanly separates the three fractions (total cation load of 7000  $\mu\text{g}$ ). Bottom panel shows an overloaded elution curve (total cation load of 12000  $\mu\text{g}$ ).

**Figure 4.** Average cation concentrations in quartz analyzed during 2009-2012 ( $n = 797$ ), expressed both in terms of mass ( $\mu\text{g g}^{-1}$ , light gray bars, left axis) and charge equivalent (meq  $\text{g}^{-1}$ , dark gray bars, right axis). Error bars show  $\pm$  one standard deviation. The total capacity of our 5 mL cation columns is 8.5 meq, and we determined that column failure occurred at  $\sim 10\%$  capacity (0.85 meq). Assuming we use 20 g of average quartz shown here ( $0.021 \text{ meq g}^{-1}$  excluding Fe, which is removed during anion column chromatography), then our columns are on average operating half-way (0.42 meq) to their failure capacity.

**Figure 5.** Histograms of Be measurements from ICP-OES aliquots taken from samples directly following dissolution. Top panel shows data for blanks ( $n = 114$ ) and bottom panel shows data for samples ( $n = 797$ ; note log scale on y-axis). Since no processing (except dissolution) has occurred at this point in the process, samples should return 100% of the expected Be. Samples containing more than 100% of the expected Be likely contain native  $^9\text{Be}$ . Thick bar shows average  $\pm 1\text{SD}$ .

**Figure 6.** Histograms of Be measurements from ICP-OES aliquots taken from samples just before final precipitation. Top panel shows data for blanks ( $n = 114$ ) and bottom panel shows data for samples ( $n = 797$ ; note log scale on y-axis). Since 6% of the sample was removed in the first set of aliquots, final yields should be 94%. Samples containing more than 94% of the expected Be likely contain native  $^9\text{Be}$ . Thick bar shows average  $\pm 1\text{SD}$ .

**Figure 7.** Final cation contents in Be fractions (from yield test data; black bars) compared to initial total cation contents in quartz (from quartz test data; gray bars; obtained by multiplying the concentration of cations in quartz by the mass of quartz used for each sample). Y-axis is in logarithmic scale.

**Figure 8.** Box and whisker plots of process blanks from three different scenarios: beryl carrier in the low-level hood ( $n = 59$ ), beryl carrier in the high-level hood ( $n = 29$ ), and SPEX carrier in the high-level hood ( $n = 22$ ). The box encloses the area between the first and third quartiles and the horizontal line represents the median. Whiskers show one standard deviation. Samples that lie outside one standard deviation from the mean are shown with an asterisk.

**Figure 9.** Blank  $^{10}\text{Be}/^9\text{Be}$  ratios from 2009-2012 from three different scenarios: beryl carrier in the low-level hood (A;  $n = 59$ ), beryl carrier in the high-level hood (B;  $n = 29$ ), and SPEX carrier in the high-level hood (C;  $n = 22$ ).

**Figure 10.** AMS  $^9\text{Be}^{3+}$  beam currents ( $n = 797$ ). Top panel shows beam currents ( $\mu\text{A}$ ) measured on the Lawrence Livermore National Laboratory AMS. Bottom panel shows sample beam currents normalized to standard beam currents.

Figure 1  
[Click here to download high resolution image](#)

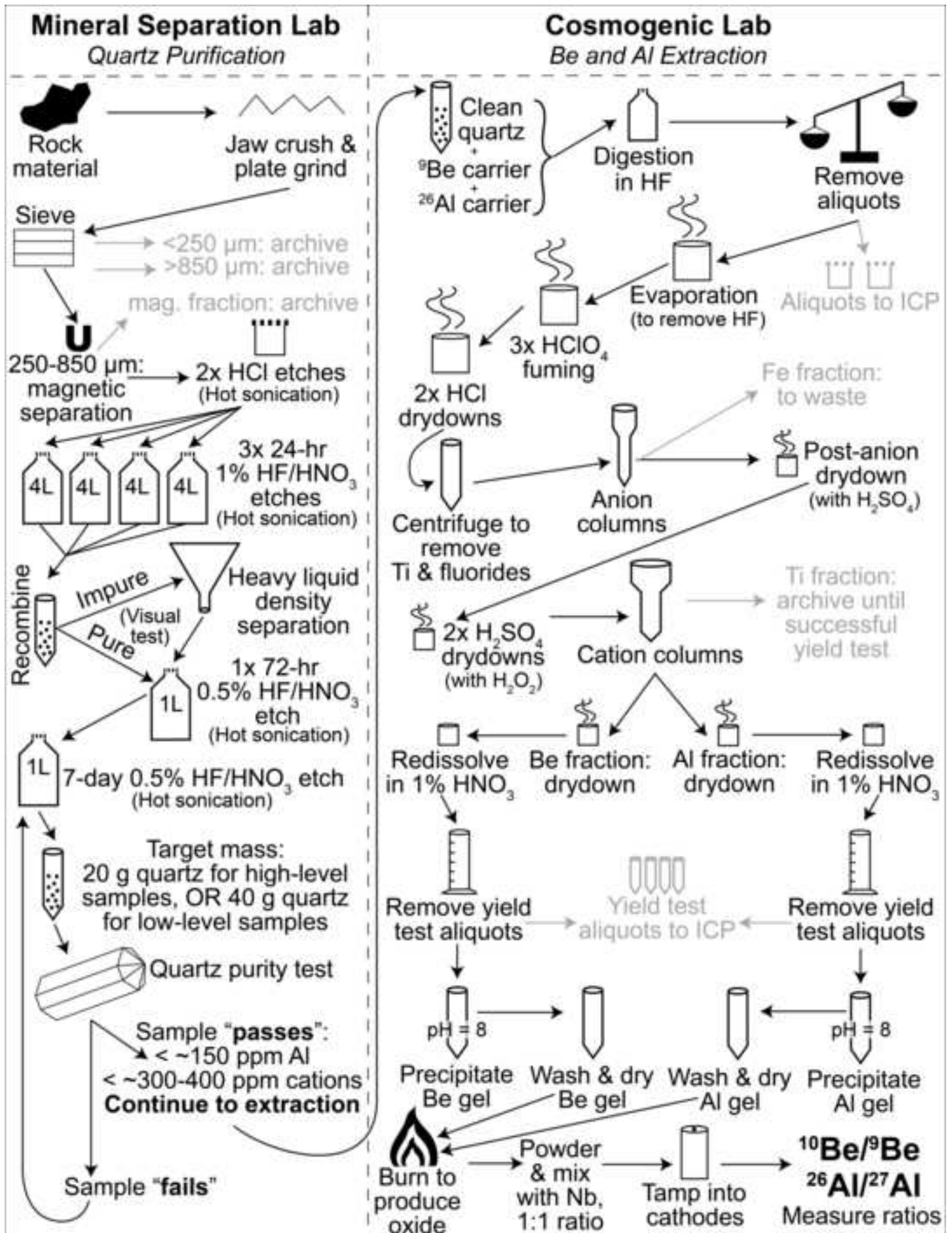


Figure2

[Click here to download high resolution image](#)

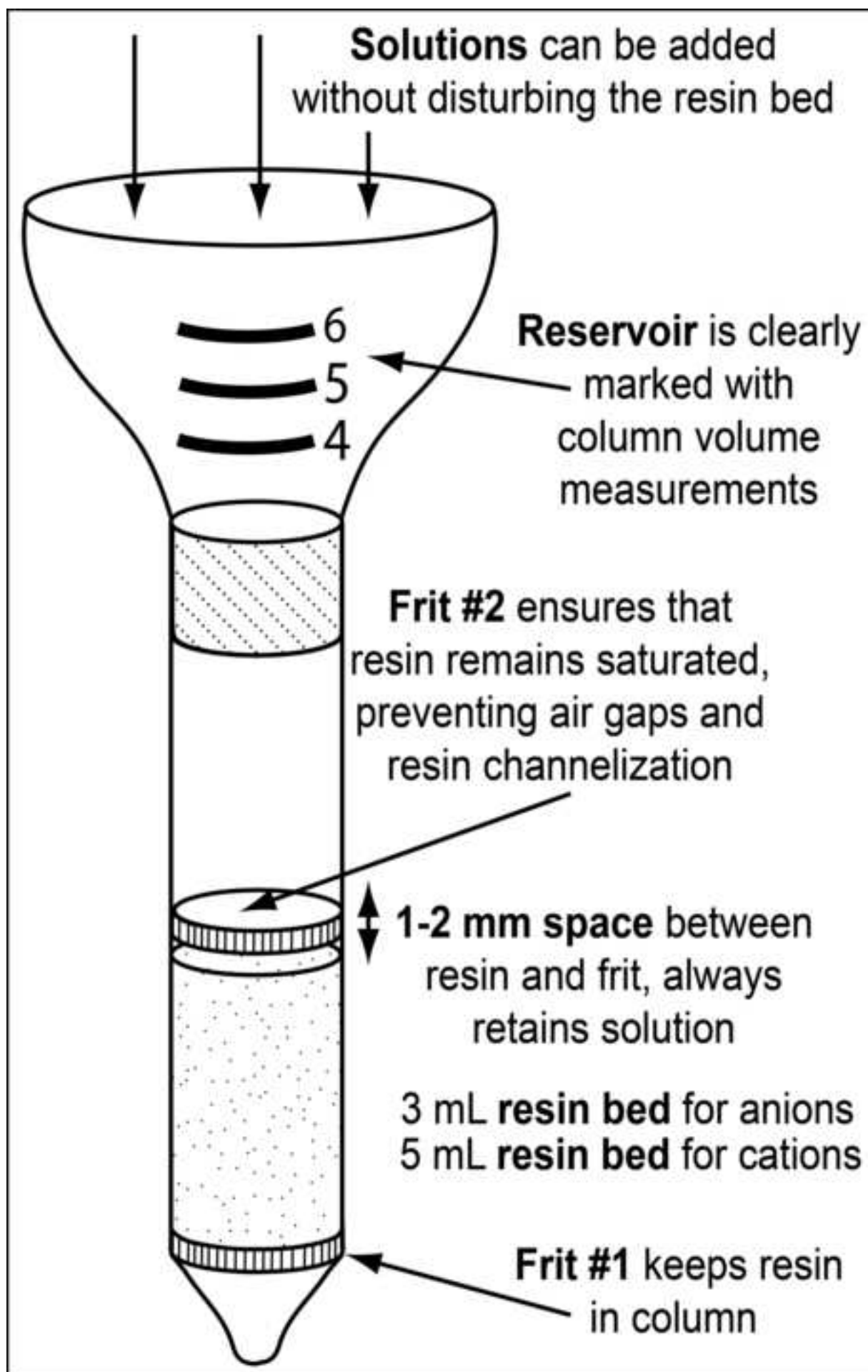


Figure3

[Click here to download high resolution image](#)

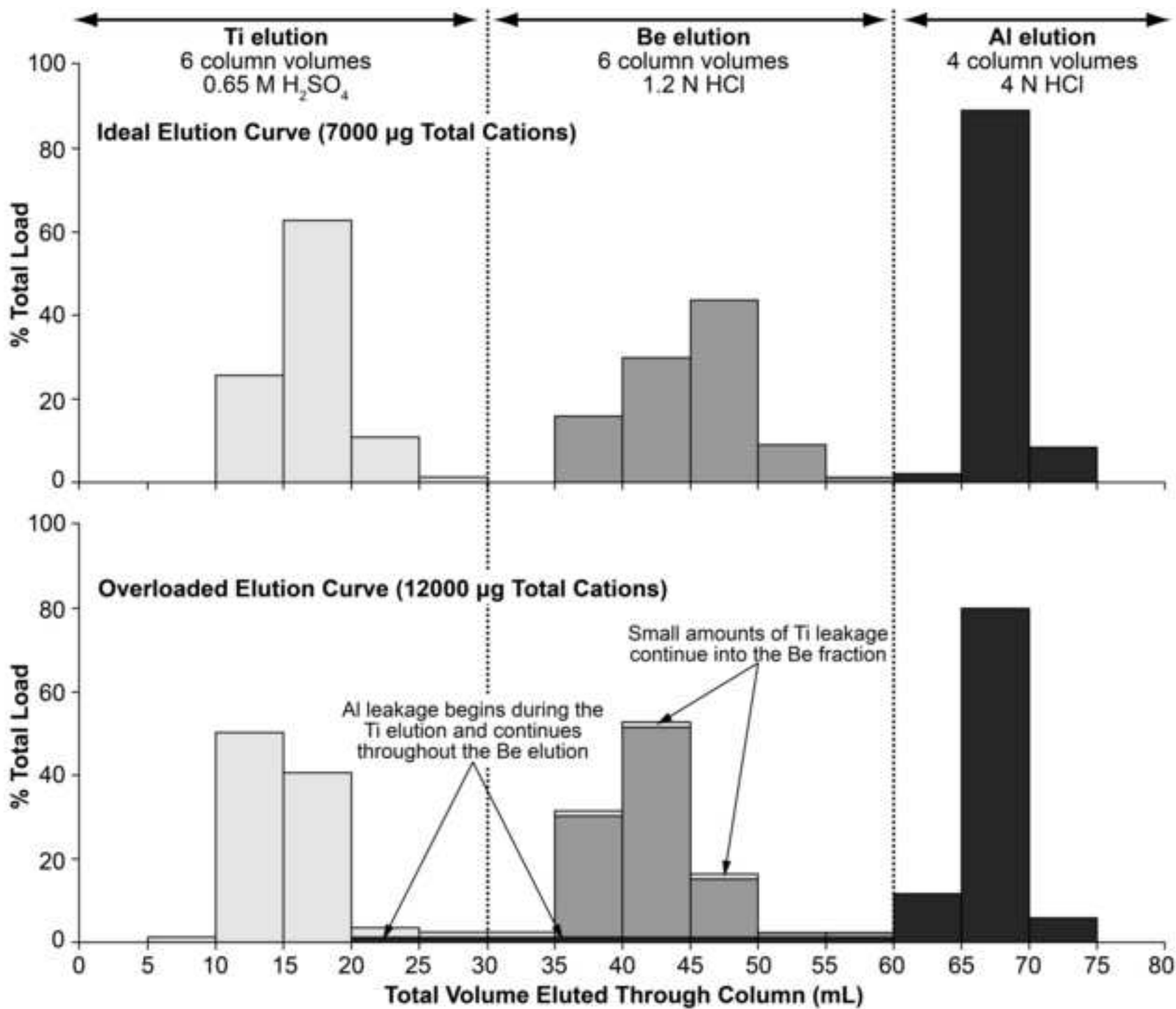


Figure4

[Click here to download high resolution image](#)

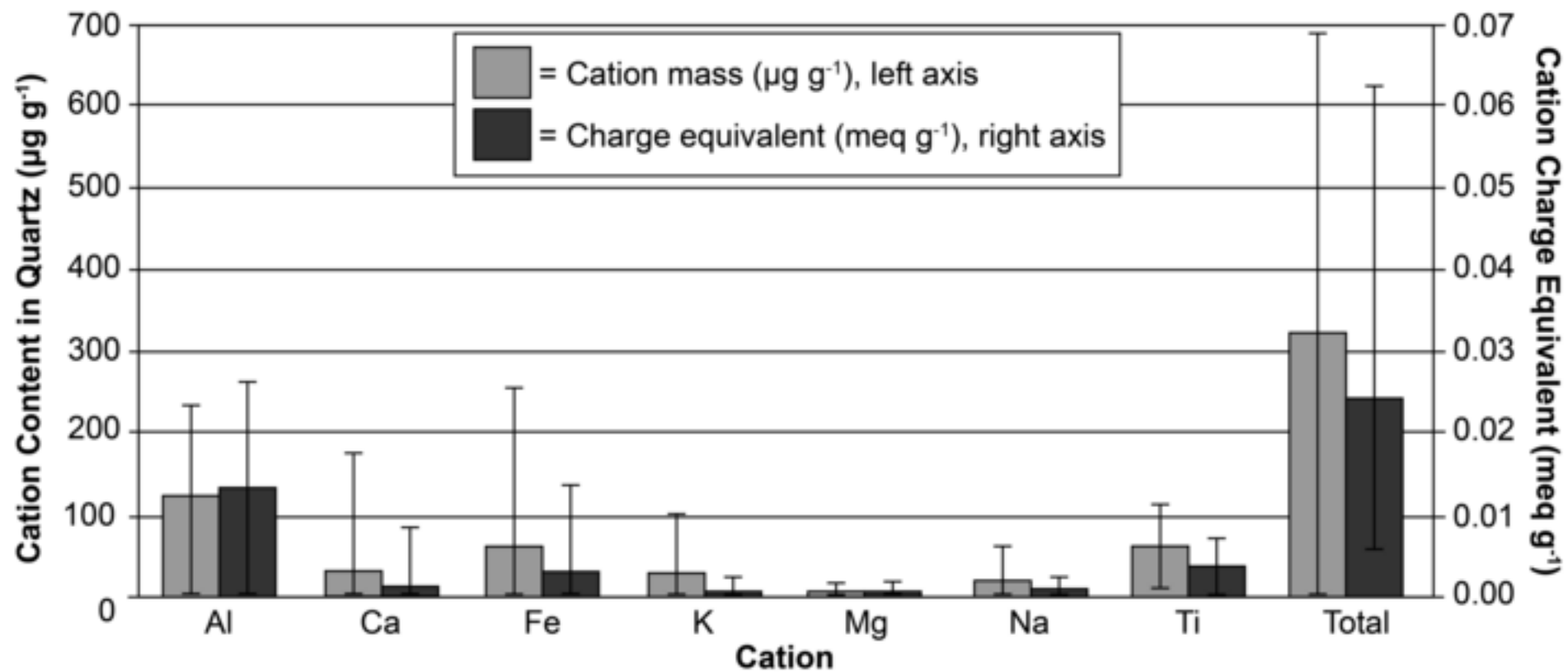


Figure5

[Click here to download high resolution image](#)

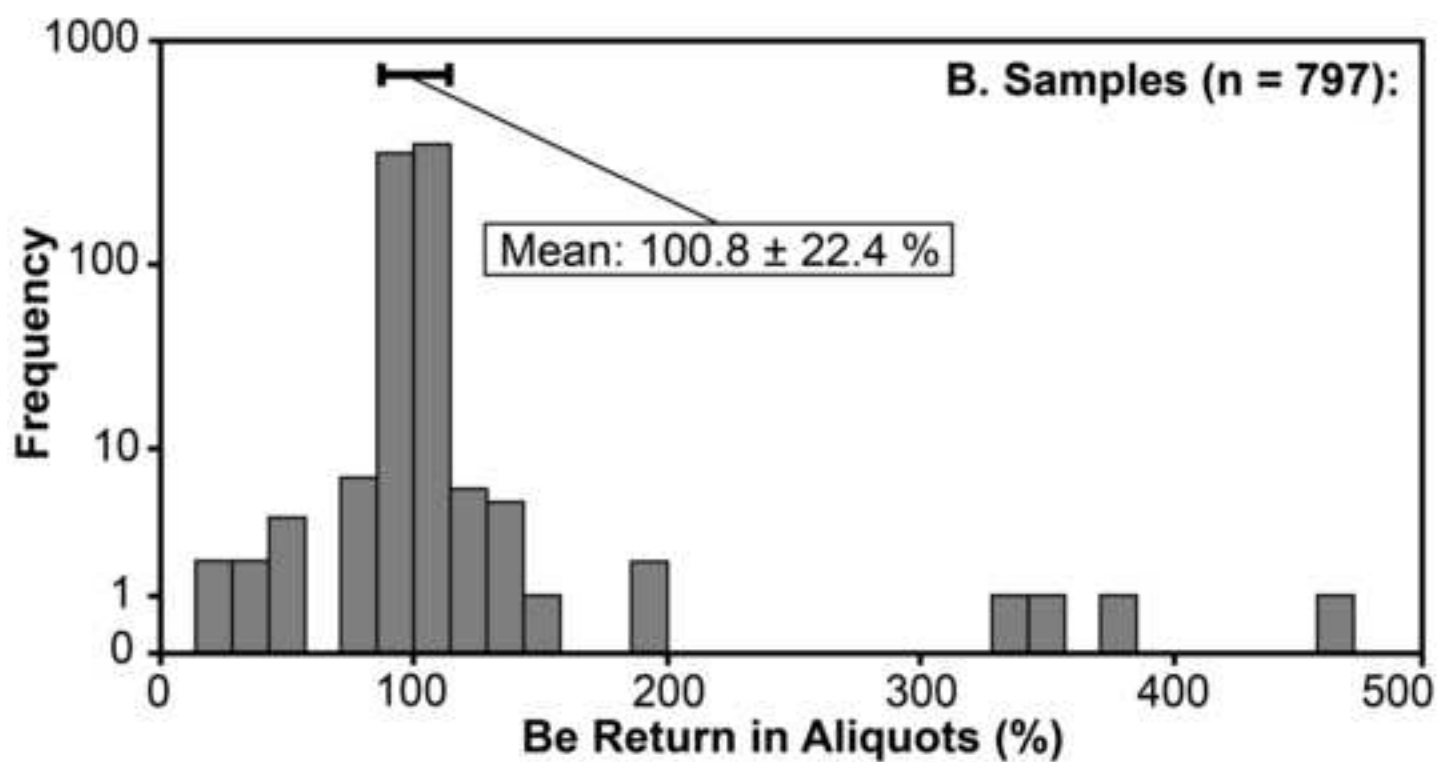
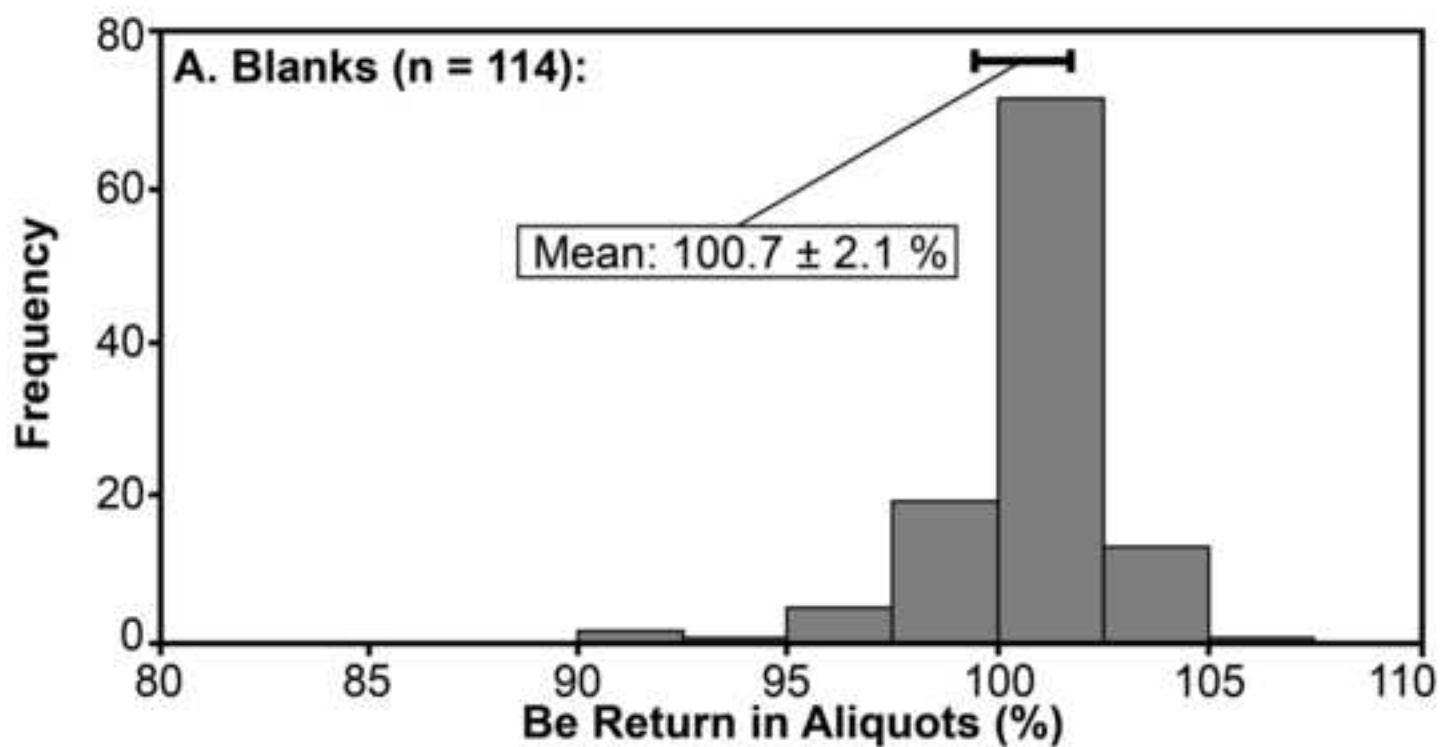


Figure6  
[Click here to download high resolution image](#)

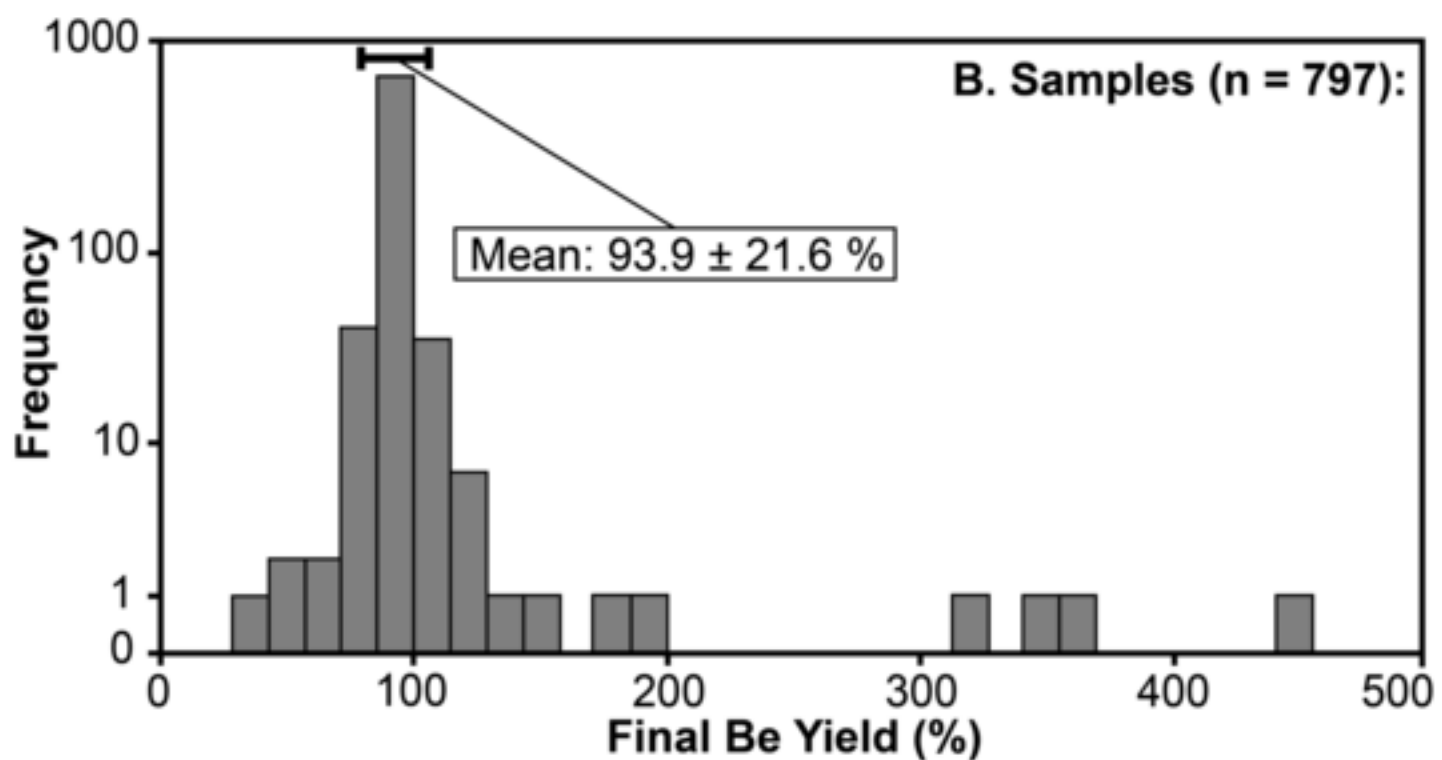
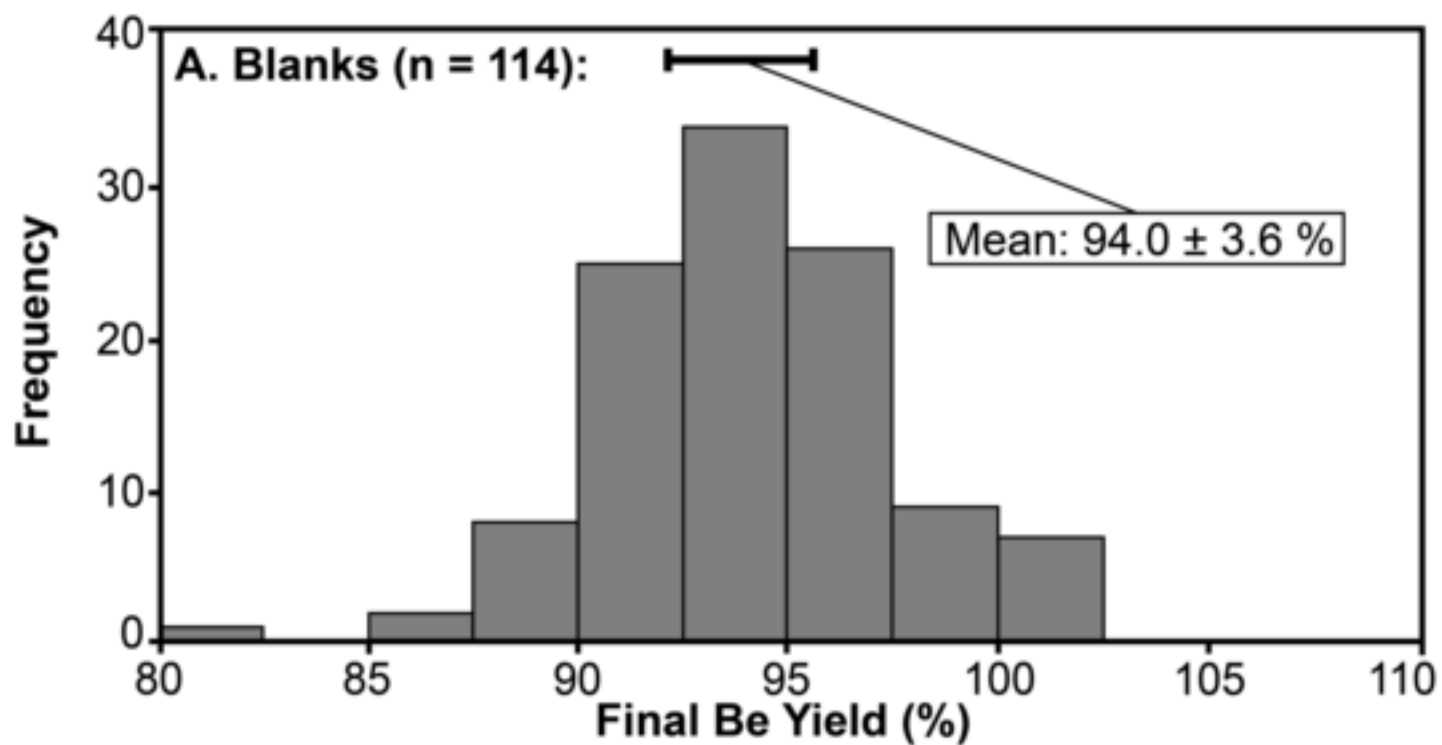




Figure7  
[Click here to download high resolution image](#)

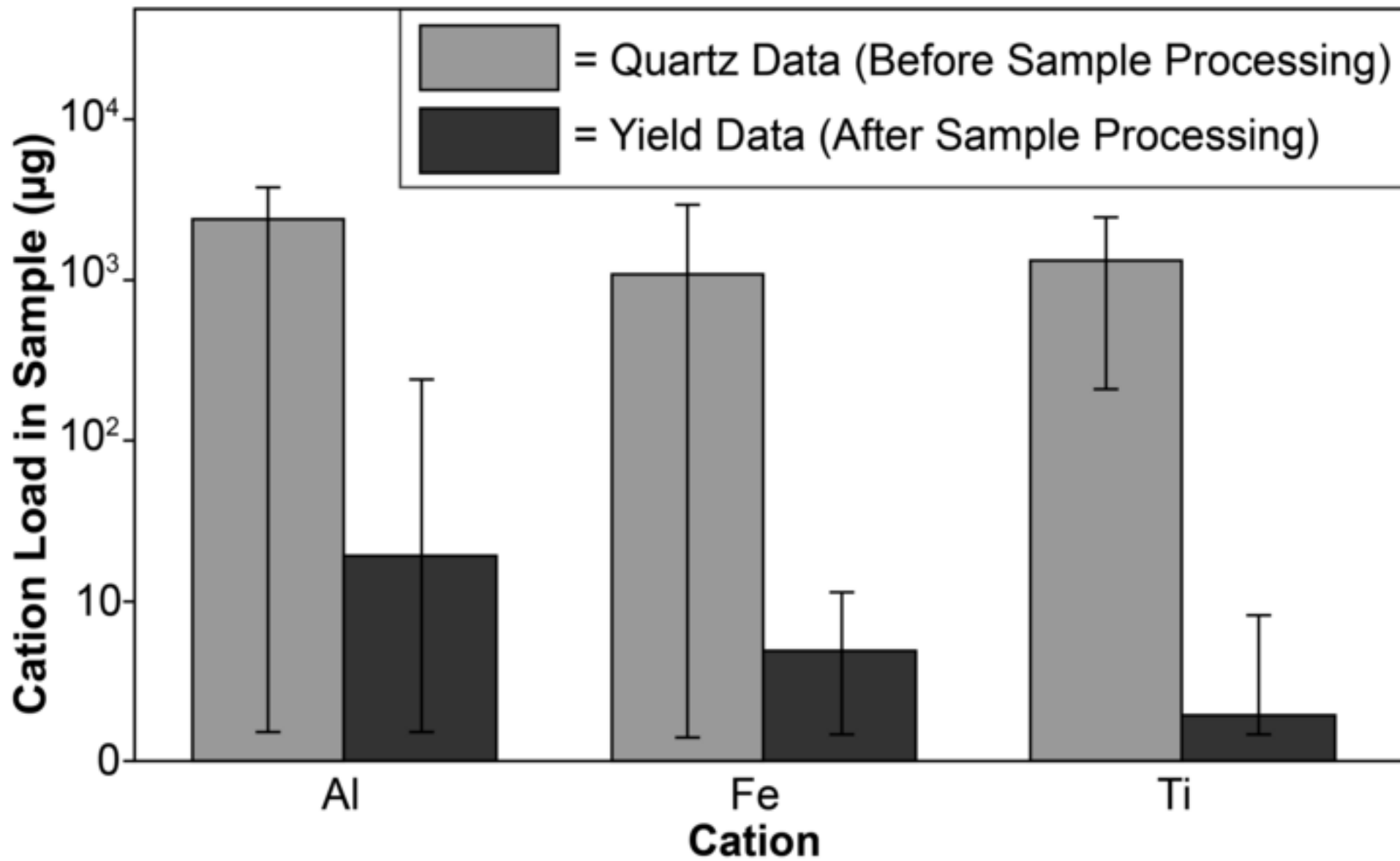


Figure8  
[Click here to download high resolution image](#)

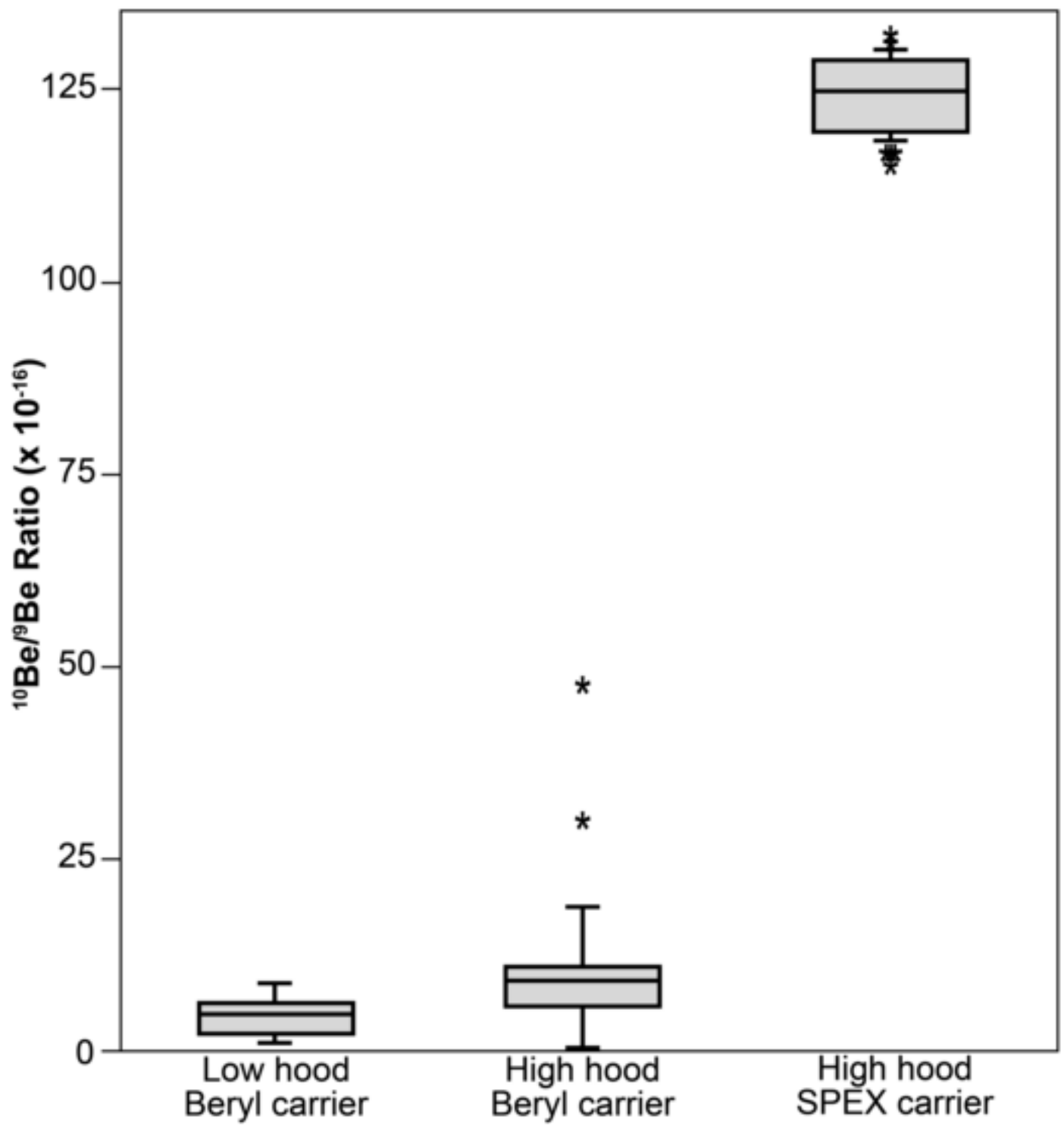


Figure9

[Click here to download high resolution image](#)

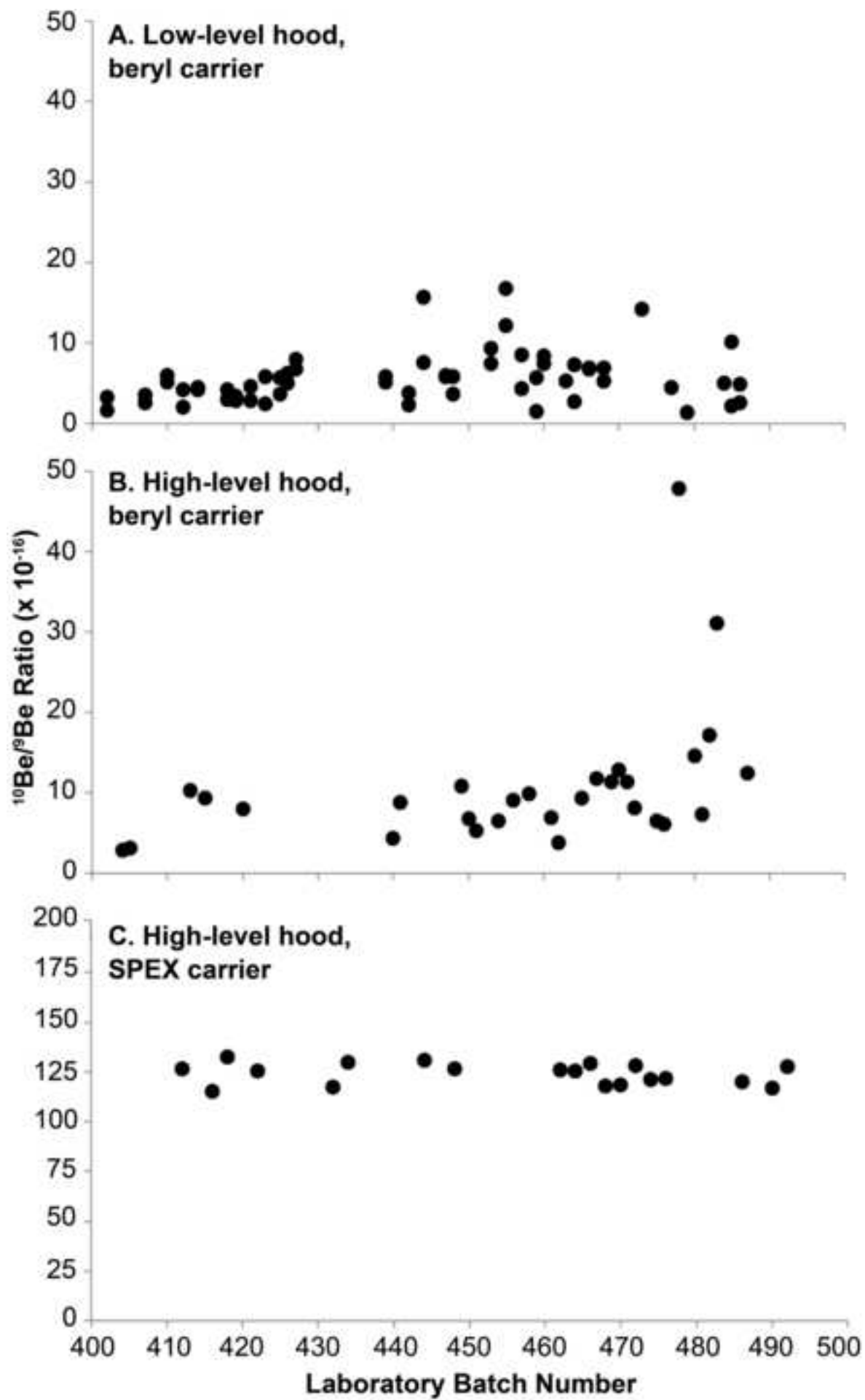


Figure10  
[Click here to download high resolution image](#)

